LASER INTERFEROMETER GRAVITATIONAL WAVE OBSERVATORY
- LIGO -
CALIFORNIA INSTITUTE OF TECHNOLOGY
MASSACHUSETTS INSTITUTE OF TECHNOLOGY

Technical Note	**LIGO-T1900649-v4**	2019/12/04

Frequency Dependent Squeezing Preliminary Optical Layout

L. McCuller, S. Biscans, L. Barsotti

Distribution of this document:

LVC

California Institute of Technology
LIGO Project, MS 18-34
Pasadena, CA 91125
Phone (626) 395-2129
Fax (626) 304-9834
E-mail: info@ligo.caltech.edu

Massachusetts Institute of Technology
LIGO Project, Room NW17-161
Cambridge, MA 02139
Phone (617) 253-4824
Fax (617) 253-7014
E-mail: info@ligo.mit.edu

LIGO Hanford Observatory
Route 10, Mile Marker 2
Richland, WA 99352
Phone (509) 372-8106
Fax (509) 372-8137
E-mail: info@ligo.caltech.edu

LIGO Livingston Observatory
19100 LIGO Lane
Livingston, LA 70754
Phone (225) 686-3100
Fax (225) 686-7189
E-mail: info@ligo.caltech.edu

http://www.ligo.caltech.edu/

1 Executive Summary

This document describes the optical layout of the A+ components comprising the frequency-dependent squeezing system for O4, as well as the mode-matching solutions for all of the relevant beam paths.

The optical components of the frequency-dependent squeezing systems are located in the HAM7, HAM8 and HAM5 chambers.

The current layout is captured in D1900436. A list of the required active electrical components is captured in E1900237. A layout of the full optical system is in D1900281.

The HAM7 chamber hosts:

- the OPOS platform (including two low-loss, small aperture Faraday Isolators (SF1 and SF2)), whose optical layout is modified with respect to the O3 layout to accommodate beams to/from the filter cavity;
- the input coupler of the ≈300m (297.85m) filter cavity (FC1);
- the suspended relay optics between the OPO and the filter cavity (ZM1, ZM2 and ZM3) and two of the suspended relay optics between the filter cavity and the OFI (ZM4 and ZM5);
- other steering optics to route control beams from the OPOS platform to the in-air tables;
- a beam diverter to send the squeezed beam to a diagnostic homodyne detector in-air.
- two WFSs in reflection of the filter cavity.

Both 532 and 1064nm beams propagates to the filter cavity, so many of the optics in HAM5 are dual coated.

The beam height on HAM7 is 5.532", defined by the center of the filter cavity optic in HSTS (as shown in G1901764). This implies that the OPOS platform needs a spacer (without a spacer the beam height is 4"), if tip-tilt suspensions are used they need a spacer, steering optics and WFSs mounted directly on the HAM7 ISI need ad-hoc posts/bases, the beam diverter needs a spacer. This height is shown in G1901764 and will be finalized from M1900157.

The HAM8 chamber Hosts the output coupler of the filter cavity (FC2), transmission QPDs in-vacuum for 1064. Relay optics carry the transmission signals to the QPDs and an in-air table.

The HAM5 chamber hosts the last suspended relay optic (ZM6) between the filter cavity and the OFI.

AWC In this preliminary design, there are three relay optics that are equipped with AWC: ZM2, ZM4 and ZM5. Double suspensions are preferred for all of the ZMs, although they are strictly necessary only for ZM2, ZM4, and ZM5.

Relay Optics Here are the characteristics of all of the relay optics. They are quoted in nominal ROC, which may potentially be offset and held at nominal by the SAMS actuators:

- ZM1: flat optic, no AWC - preferably a double suspension, it could be a tip-tilt (modified for large AOI) if needed;
- ZM2: curved optic (0.85m ROC nominal, concave) with AWC, it must be a SAMS;
- ZM3: flat optic, no AWC - preferably a double suspension, it could be a tip-tilt if needed;
- ZM4: flat optic with AWC, it must be a SAMS;
- ZM5: curved optic (3.4m ROC nominal, concave) with AWC, it must be a SAMS;
- ZM6 (in HAM5): flat optic, no AWC - preferably a double suspension, it could be a tip-tilt (modified for large AOI) if needed.

Two in-air tables are part of this system:

- SQZT8 (the equivalent of the current ISCT6) which will provide the pump and control fields via optical fibers to the OPO;
- SQZT7 (the equivalent of the current SQZT6), which will host diodes used for control and monitoring.

1.1 Parameter Tables

Tables 1, 2, 3 and 4 given the designed beam parameters and Gouy separations along the suspended optic paths of the squeezer, filter cavity and relay optics.

	$2w$ beam $\varnothing$[mm]
FC2	28.601
FC1	18.497
ZM3	9.836
ZM2	4.954
ZM1	0.411
ZM4	1.933
ZM5	3.843
ZM6	2.121
SRM	4.284

Table 1: Beam Diameters for the suspended optics cavity and relay optics for frequency dependent squeezing.

Gouy Shifts [deg]	(A)	(B)	(C)	(D)	(E)	(F)
(A) FC2	0	-49.7166	-50.1608	132.672	37.8955	108.933
(B) FC1	49.7044	0.0122071	-0.444258	-177.611	87.6121	158.649
(C) ZM3	50.1608	0.456465	0	-177.167	88.0564	159.093
(D) ZM2	-132.672	177.623	177.167	-0	-94.7767	-23.7396
(E) ZM1	-37.8955	-87.5999	-88.0564	94.7767	0	71.0371
(F) ZM4	-108.933	-158.637	-159.093	23.7396	-71.0371	-0

Table 2: Gouy Phase separation table for filter-cavity side suspended optics, calculated from filter cavity beam propagation, Y-axis beam parameter. Diagonals show phase advance through thick optic.

Gouy [deg]	(A)	(B)	(C)	(D)	(E)	(F)	(G)
(A) FC2	0	-49.7166	108.933	91.0859	-36.1331	-50.6117	-54.5915
(B) FC1	49.7044	0.0122071	158.649	140.802	13.5835	-0.895136	-4.87491
(C) ZM4	-108.933	-158.637	-0	-17.8467	-145.066	-159.544	-163.524
(D) ZM5	-91.0859	-140.79	17.8467	-0	-127.219	-141.698	-145.677
(E) ZM6	36.1331	-13.5713	145.066	127.219	0	-14.4786	-18.4584
(F) OFI/TFP/	50.6117	0.907343	159.544	141.698	14.4786	0	-3.97978
(G) SRM	54.3756	4.67119	163.308	145.461	18.2424	3.76384	0.215932

Table 3: Gouy Phase separation table for interferometer-side suspended optics, calculated from filter cavity beam propagation, Y-axis beam parameter. Diagonals show phase advance through thick optic.

Beam Q's	FC side
FC2	W=14.30mm, Z=-297.9m , 1/R=-1.953mD, W0=9.249mm, ZR=252.6m
FC1	W=9.249mm, Z= 0.000m , 1/R= 0.000D , W0=9.249mm, ZR=252.6m
ZM3	W=4.918mm, Z=-1.183m , 1/R=-845.3mD, W0=81.45um, ZR=19.59mm
ZM2	W=2.477mm, Z= 595.4mm, 1/R= 1.678D , W0=81.45um, ZR=19.59mm
ZM1	W=205.6um, Z= 20.26mm, 1/R= 1.337D , W0=202.8um, ZR=121.4mm
ZM4	W=966.8um, Z= 1.285m , 1/R= 530.6mD, W0=545.2um, ZR=877.6mm
ZM5	W=1.922mm, Z= 2.967m , 1/R= 309.9mD, W0=545.2um, ZR=877.6mm
ZM6	W=1.061mm, Z= 1.551m , 1/R= 437.4mD, W0=601.4um, ZR=1.068m
OFI/TFP/	W=1.753mm, Z= 2.923m , 1/R= 301.8mD, W0=601.4um, ZR=1.068m
SRM	W=2.142mm, Z= 3.651m , 1/R= 252.3mD, W0=601.4um, ZR=1.068m
Beam Q's	IFO side
FC2	W=14.30mm, Z=-297.9m , 1/R=-1.953mD, W0=9.249mm, ZR=252.6m
FC1	W=9.249mm, Z=-2.224m , 1/R=-449.6mD, W0=81.45um, ZR=19.59mm
ZM3	W=4.918mm, Z=-1.183m , 1/R=-845.3mD, W0=81.45um, ZR=19.59mm
ZM2	W=2.477mm, Z=-1.478m , 1/R=-671.9mD, W0=202.8um, ZR=121.4mm
ZM1	W=205.6um, Z= 20.26mm, 1/R= 1.337D , W0=202.8um, ZR=121.4mm
ZM4	W=966.8um, Z= 1.285m , 1/R= 530.6mD, W0=545.2um, ZR=877.6mm
ZM5	W=1.922mm, Z=-3.242m , 1/R=-278.3mD, W0=601.4um, ZR=1.068m
ZM6	W=1.061mm, Z= 1.551m , 1/R= 437.4mD, W0=601.4um, ZR=1.068m
OFI/TFP	W=1.753mm, Z= 2.923m , 1/R= 301.8mD, W0=601.4um, ZR=1.068m
SRM	W=2.170mm, Z= 4.983m , 1/R= 170.4mD, W0=844.0um, ZR=2.103m

Table 4: Full beam parameters on either side of each suspended optic. Calculated from the propagation of the filter cavity mode, Y-axis beam parameter. The sign of the Z and 1/R parameters is for a beam traveling from FC to IFO.

2 Overview

2.1 Principle Requirements

ASC Gouy Phase Separations For the suspended optics relaying the squeezed beam between the OPOS, FC1 and OFI, the Gouy phase separations must be near enough 90 degrees that the sensing and actuation is far from degenerate.

Active Wavefront Control In as many paths as possible, wave front control is desired to achieve $> 96\%$ mode matching or better. E1900257 details these requirements. In short, they are to have sufficiently large beams on the wavefront-control enabled optics ($\varnothing >$ 4mm at 1064nm), and for the Gouy-phase separation to be ideally by 45 degrees between the AWC optics. T1900144 shows that for sequentially placed AWC systems, large spacing are necessary to actuate the wavefront in both quadratures. A single HAM ISI table is not a sufficient baseline for strong 2-quadrature actuation. This motivates the cris-crossed beam aesthetic achieved in the current layout.

AWC requirements can be at odds with ASC requirements, however each squeezing beam path has 3 relay suspensions and optics, ZM1-ZM3 to the filter cavity and ZM4-ZM6 to the interferometer. With the additional suspensions it can be possible (in principle) to achieve acceptable Gouy phase separations for both uses. Unfortunately, the AOI is constrained to be large for some of the relay optics.

Astigmatism For any optic with some focussing power, AWC or not, the AOI on the optic must be small enough to prevent astigmatism. In this document, the astigmatism is measured as "Self-overlap", the coupling efficiency of the X-transverse beam parameter with respect to the Y-transverse beam parameter. This is held to be as low as possible, and must stay above 99%. In the future, it may be possible to plot the phasing of HG02 mode between X and Y beam parameters, this could help indicate which downstream optic is best suited for correcting the astigmatism.

Dual 1064 and 532 control The filter cavity must have both 532 and 1064 beams propagating to it. These must be stacked on a dichroic beamsplitter. While the 1064 SQZ beam must be well mode-matched, the requirements on the 532 are less (set arbitrarily to 90%). The 532 will only be used for length sensing and stabilization for lock acquisition and diagnostics of the 1064 beams. The strong lens on the AR surface of the filter cavity optic causes differential lensing of the 532 path. This causes the telescope in the relay optics to be sub-optimal for the 532 beam. Furthermore, displacement of the filter cavity axis on FC1 and FC2 will cause the 532 and 1064 beam centers to offset on the OPO suspension.

Fitting on the OPOS platform The suspended platform for the OPO was optimized for space on the HAM6 ISI. It appears sufficient for implementing FDS, but it will be a tight fit for optics. New components include an additional Faraday isolator, and the filter cavity green sensing beam (FCGS).

Accessability and Reliability The auxiliary beams should be accessible and adjustable for commissioning and maintaining operation with the SQZT7 table. This has led to the placement of the SQZT7 table aside the +Y door, which will be fixed in place once attached to the filter cavity beamtube. This will prevent the need to realign, but it also requires a long baseline for the auxiliary beams to traverse the ISI.

Unfortunately, the long baseline requirements of the AWC implementation require a tangle of beams in the center.

Decoupled Mode Matching Due to the use of a Faraday to circulate the Squeezing path between the filter cavity reflect and interferometer, the mode matching telescope towards the cavity couples these two paths in a complicate manner. If the initial solution is established in the optics lab, ideally, changes to improve matching to the filter cavity should not too strongly affect matching to the IFO. See Sec. 4.1.

Similarly, lenses in paths carrying both 1064 and 532 beams should be avoided or should not be necessary to move to tune mode-matching.

2.2 HAM7 Layouts

Figures 1, 2, and 3 show the current layouts of the HAM7 beams and a view of the layout of the OPO platform. These layouts every designed beam path. The mode matching solutions and explanations for the suspended squeezing paths is in sec. 3.1.

2.3 HAM8 Layout

The beam is 30mm ⌀on FC2, reduced by the AR-side lens, but needs and extension before hitting first relay optic.

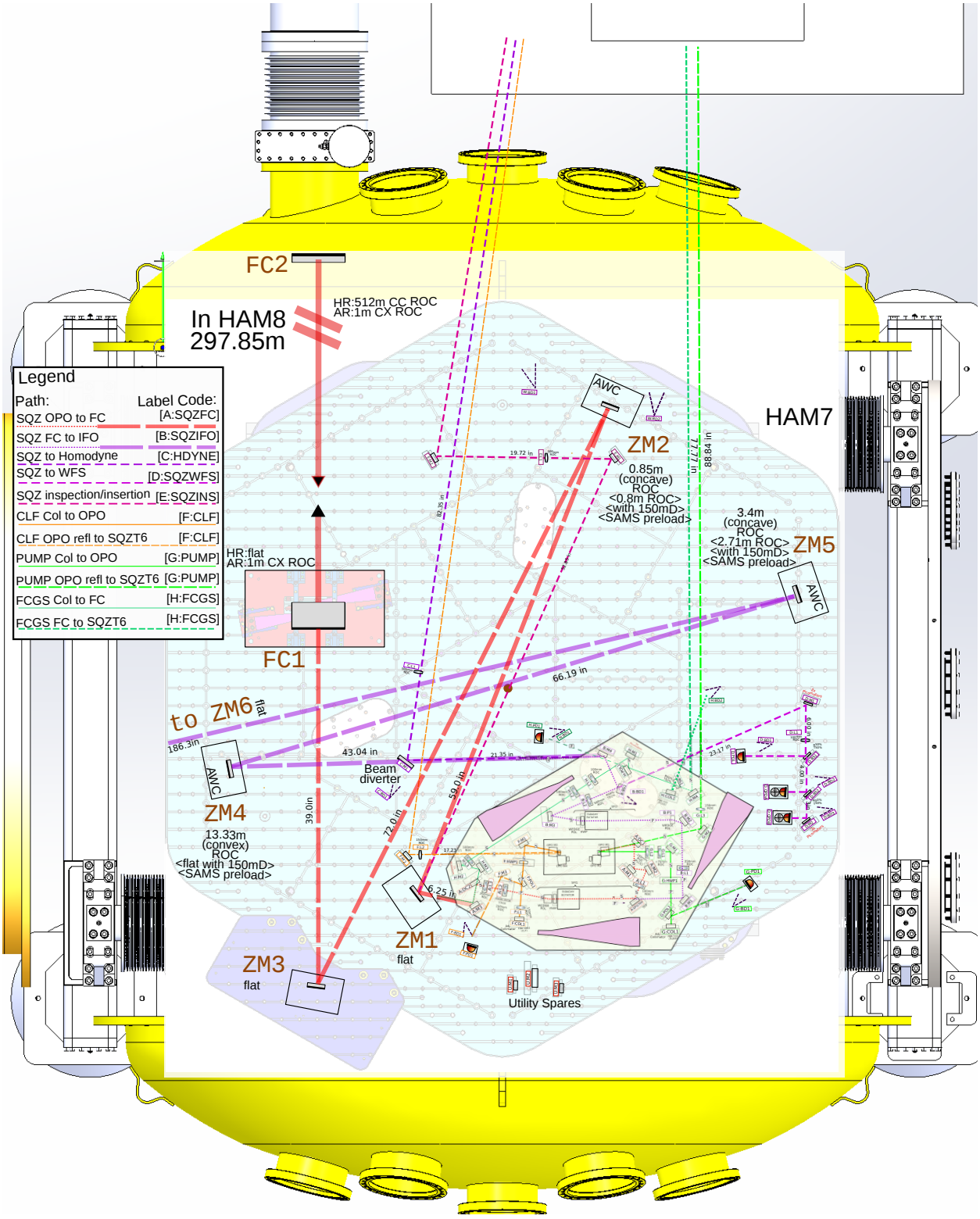

Figure 1: The beam layout on HAM7. The thick red and purple beams indicate the primary paths between suspensions for squeezing. The lengths indicated are from this cartoon, and will be pinned down with a chamber model. The lens positions assume the given path lengths. In sec. 2.4 the various auxiliary beams and labeling scheme are described. The ZM mirror ROCs are nominal working values. The purchased values will be based on the chosen AWC system.

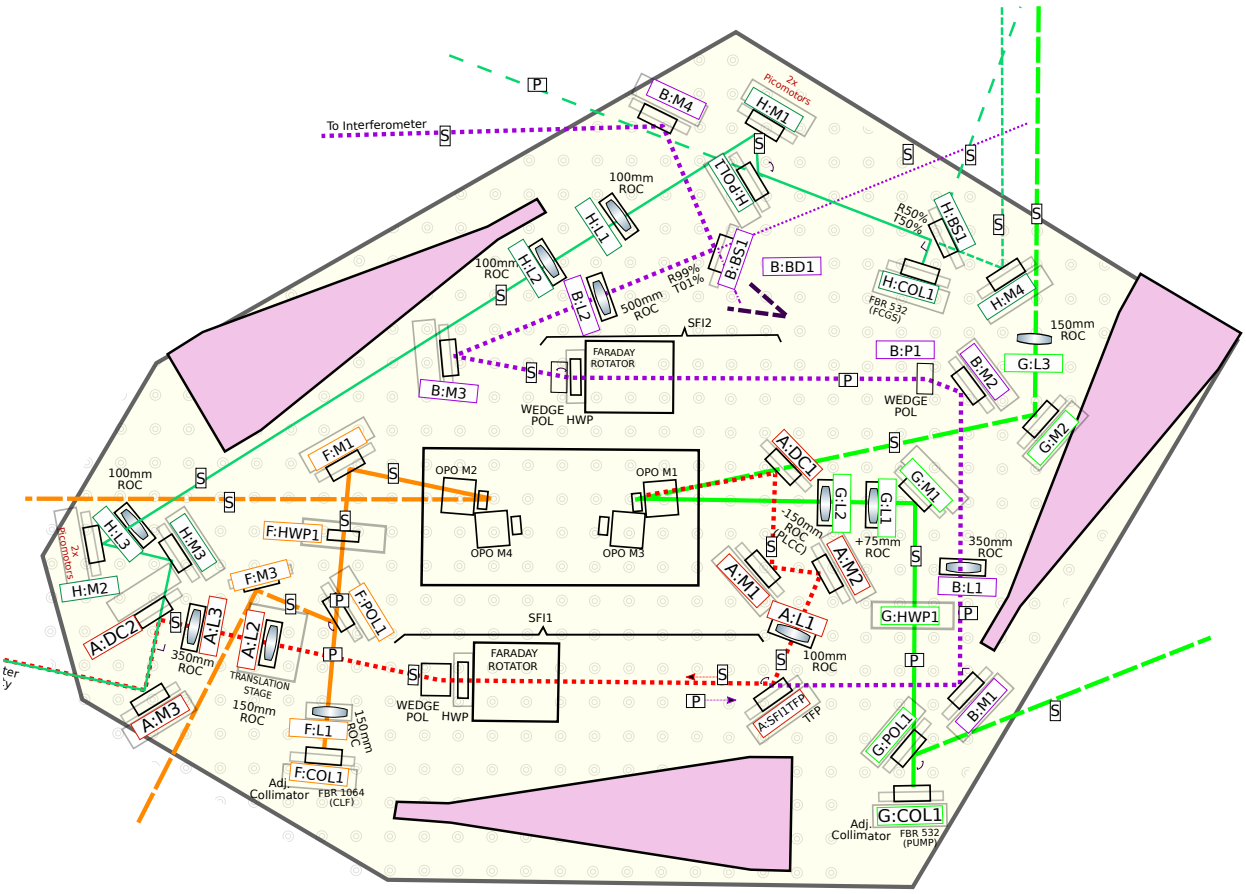

Figure 2: The beam layout on the OPOS platform (the VOPO injection platform, VIP). It follows the same labeling scheme as Fig. 1, elaborated in Sec. 2.4. This is an overlay of the solidworks model of fig 3, which includes calculated lens positions, optic labels and beam polarizations. Alternate configurations are shown in sec. **??**. Some of the difficulties of this design are outlined in 2.5

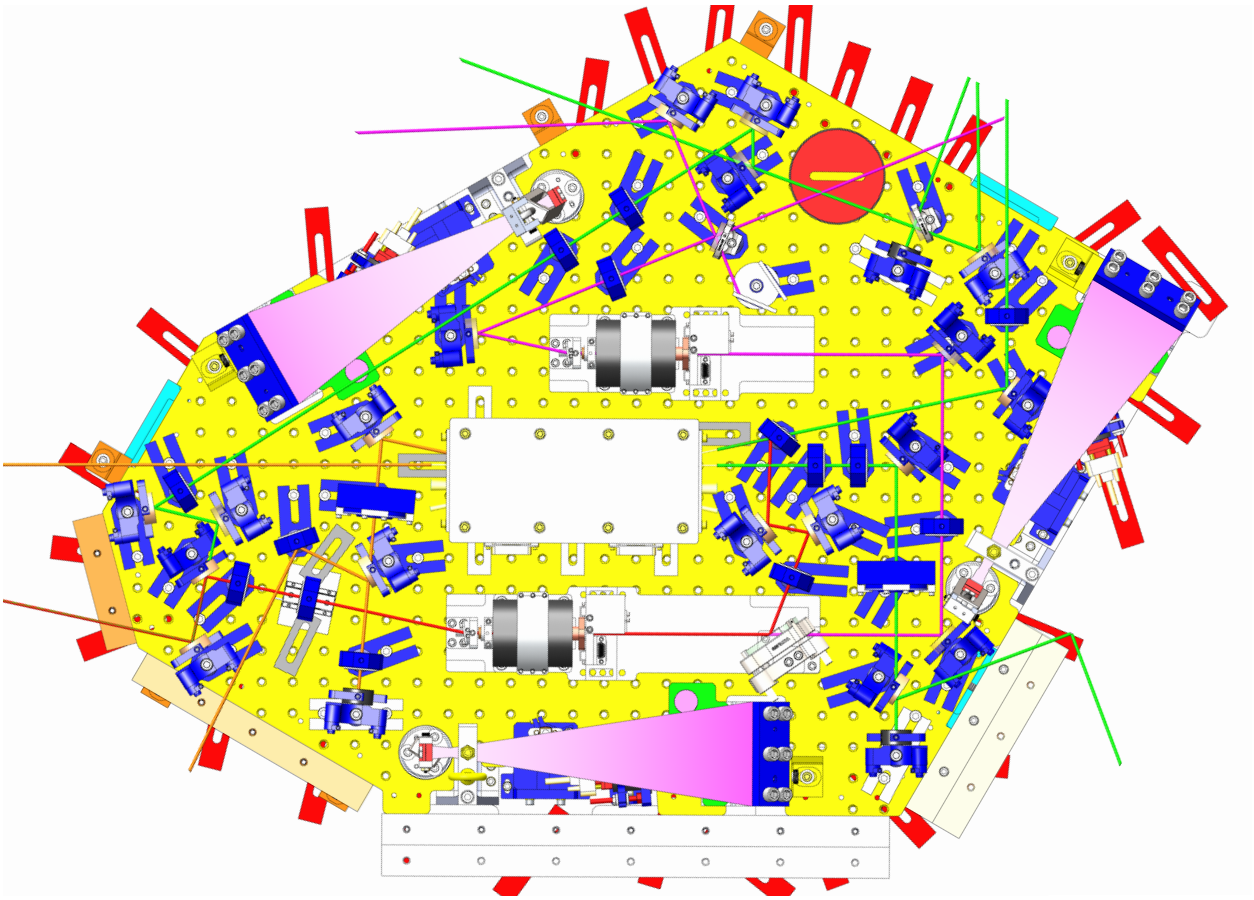

Figure 3: Solidworks model of the beam layout on the OPOS platform (the VOPO injection platform, VIP). NOTE, not everything is fully completed. Lenses and picomotors shown in Fig. 2 are not yet placed, nor are dogs. Faraday elements added as placeholders, to be characterized/tuned independently and dropped on as sleds.

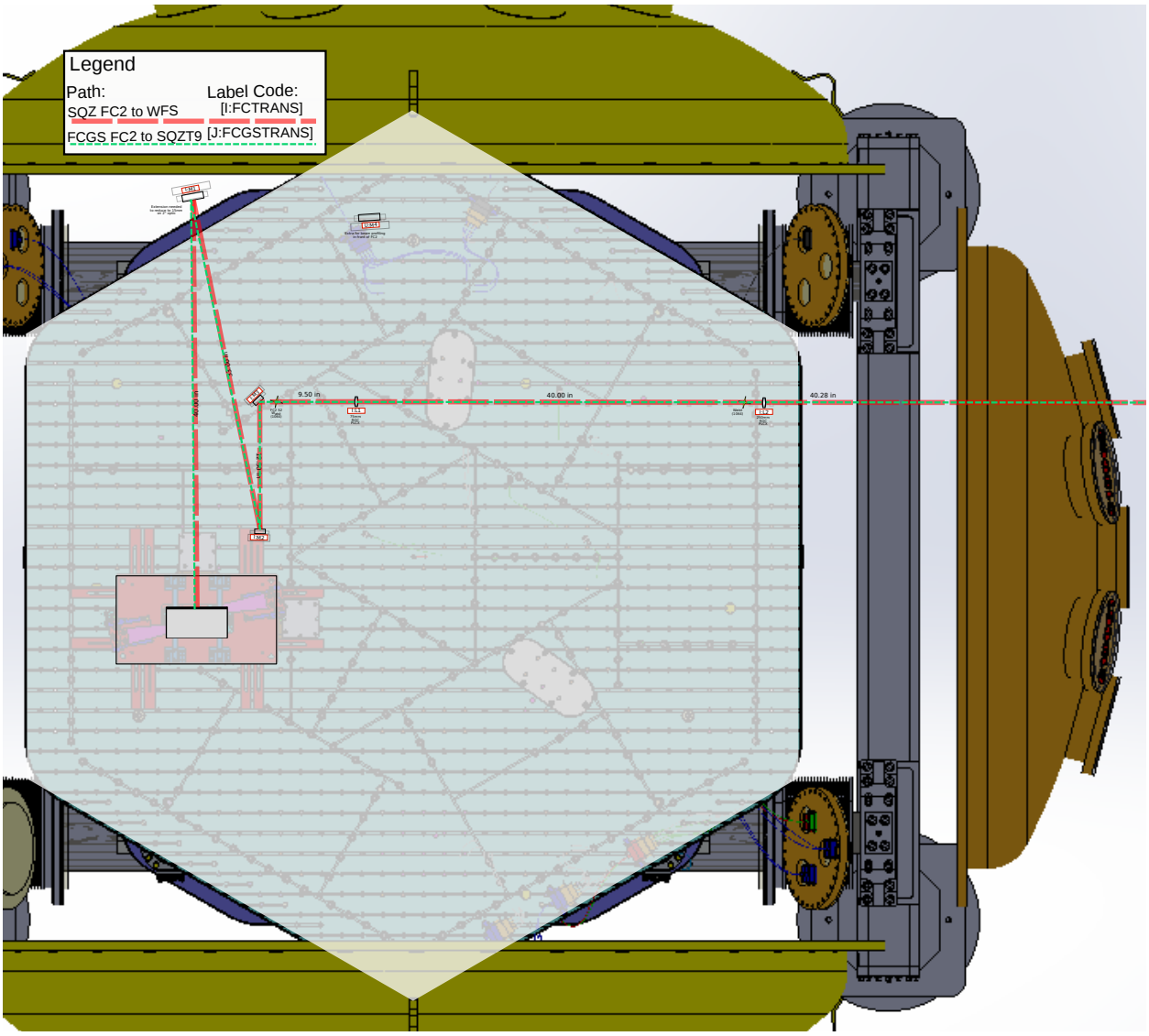

Figure 4: The beam layout on HAM8. This is primarily a telescope between the FC2 lens and the "collimating" lens I:L1. That lens is set to create a soft waist for a telescope for 1064 QPDs. The 532 FCGS transmission is split off on I:DC1 and has a separate lens J:L1 to collimate it and send it to out for transmission power monitoring.

2.4 Description of paths

Squeezing Path In overview, the squeezing starts from the OPO, travels through the SFI1 Faraday to the linear filter cavity, as the SQZFC path, reflects from the cavity, then the SFI1 Faraday is used to circulate the beam towards SFI2, which it passes through as the SQZIFO path and is beamed to the interferometer. On its way, 1% of the squeeze beam is picked off for wavefront sensing and (potentially) length control along the SQZWFS path. The necessary fields are also available in the interferometer, but the SQZWFS will provide cleaner dedicated readouts until the control scheme is demonstrated. Fig 5 shows this path in a simplified form.

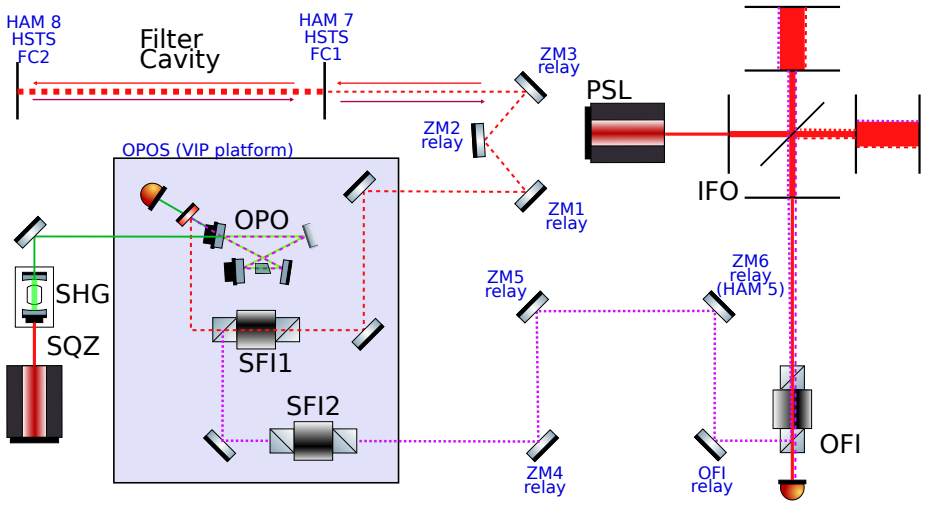

Figure 5: Cartoon of the Faraday naming and beam sequence for the squeezing path to filter cavity and interferometer.

The squeezing path starts from M1 of the OPO. The 532 PUMP light reflection is initially stacked on top, and stripped from A:DC1. In the previous OPO suspension, more dichroics were included to further strip the 532 light. Now there is much less space. A:M1 and A:M2 could potentially do this, but the FCGS light is added later. In this case M1 and M2 allow some steering into the Thin Film Polarizer of the SFI1 Faraday used as a circulator for the squeezing beam with the filter cavity. Since the squeezing is S-pol from the cavity, this avoids a waveplate in the O3 implementation. M1 and M2 could be removed and the DC1 dichroic used to steer. This will cause an AOI of 29 degrees on the dichroic. The existing M1 and M2 steering also allows the DC1 to reasonably be on a lens mount to provide space for the SFI2.

From the TFP, the beam is passed through the SFI Faraday. A wedge polarizer with 12 degrees deflection angle in S-pol is assumed on the output of the Faraday. The existing lens translation stage remains to provide some wavefront control on the VIP. As detailed in sec. 3.1, the filter cavity telescope is overconstrained to include two instances of AWC, so the lens stage may provide some actuation of the second DOF. This has not yet been fully studied.

From the stage, the beam is stacked with the 532 sensing field via A:DC2. This is them passed to the filter cavity by ZM1-3. Shown in Fig. 1 is an additional SQZINS path, available by deflecting ZM1 from ZM2. This path is not necessary for operation. It is provided to give

a simple means of monitoring the transmission of the IFO beam through the OFI, SFI1 and SFI2. This will allow optimizing the Faradays for isolation, in hopes to remove 1 and reduce the loss in the future. It will also allow commissioning tasks that require beam injections, potentially for transfer functions or phase cameras, without the complexity of using the OPO system as has been previously done.

OPO Pump path The pump path is the 532 beam that powers the OPO squeezing. It must be mode matched to the cavity, and read in reflection. The reflection beam is stacked with the squeezing beam, and the two are immediately separated with a dichroic optic. The reflection beam is then re-collimated once large enough and directed out of a window.

One issue in the path is that the fiber delivery to the OPO changes due to variations in the spacing between the fiber and lens of the collimator. Due to the even tighter layout, adjustable/correctable collimators are desired for O4.

OPO CLF path The CLF path injects the sensing field to the OPO using M2 rather than M1 of the OPO cavity (see the final optical design T1700104). The CLF must then be read in reflection for the control scheme. A transmission signal of the OPO pump is also carried with the CLF REFL path.

Filter Cavity Green Sensing (FCGS) The filter cavity length control with primarily be in 1064, as that provides a better witness of the SQZ field and lower phase noise, but observing and controlling the cavity in 532 is useful for diagnostics, alignment and stabilizing the cavity during lock acquisition and commissioning.

To sense the cavity, the 532 Filter Cavity Green Sensing field is stacked with the squeezing field and propagated to the cavity. The FCGS stacking is done on the VIP platform to keep its alignment as consistent with the squeezing field as possible. Although not currently included, having the lowest noise injection source will also provide the best reference to stabilize the cavity axis if 532 WFS are ever used (they would be done in-air if so). The stacking is performed using penultimate dichroic optic on the platform (A:DC2). A beamsplitter is used to pick off the REFL beam and direct it to SQZT7. Some of the REFL beam will return through the fiber to its source SQZT8. PDH could be read there, but backscatter from the fiber is a concern, so that is not planned.

2.5 VIP Layout Concerns

The layout as given is designed largely to minimize the number of used optics. Which also minimizes the number of components requiring setup. This may not be a desirable tradeoff in the event that it compromises reliability.

FCGS and SQZ coalignment The differential lensing of the FC1-AR surface between the SQZFC and FCGS beams will cause differential shifts of the beam propagation axis if

the beam is not centered on the FC1 optic. This may get large enough to cause clipping on the FCGS path or otherwise cause confusion.

Use of (fixed) lens mounts for mirrors on VIP For space, some of the mounts on the VIP platform are smaller fixed mounts such as lens mounts or beamsplitter mounts. This may frustrate alignment, particularly if it must be done in-chamber. Some elements of the current Fig. 2 layout may be superseded by the design of Fig. **??** to provide adjustability at the appropriate points. That layout has not yet been configured in solidworks or mode-matched.

2.6 HAM7 Layout Concerns

Use of 1in optics on ISI The CLF REFL beam and SQZ beam after the diverter use some 1in relay mirror and 1in collimating lenses. Additionally, the WFS uses 1in optics in its telescope. As the VIP platform of the OPOS is re-balanced, some of the alignments along these auxiliary paths may change. The 1in optics are all within 1m of the platform. The platform is approx .3m from its center to earthquake stops, which provide ±1mm of freedom, worst case (we monitor the OSEMs during balancing). This gives ±3mrad of variability in the output alignment. Over the 1m baseline, this corresponds to ±0.12in of deviation on the auxiliary steering optics.

The lenses could cause large deflections even for that defelction, however since they are designed to collimate, their focal lengths are all longer than their distance to the platform, and so that will conver the deflections to translations and actually reduce any pitch/yaw from the platform.

2.7 Required new mounts and mechanics

SFI Faradays The footprint of the SFI Faradays will have to be compatible with the VIP layout, beampath, dogs for mounting, and some obstructions such as the earthquake stops.

Shorter dogs The SFI1-2 faradays will be delivered on sleds, and the spacting to the OPO is limited (see sec C). Shorter dogs will be necessary to clamp in the spacing between SFI1 and the OPO.

adjustable collimators The current vacuum fiber patch cords and feedthroughs, particularly in 532, vary in their mode output from fiber-to-fiber. This is because the fiber tip position can vary some ±20um, enough for the collimator to not output a collimated beam. I propose that collimators with adjustable lens spacing be used to provide consistent mode output from fibers.

VIP wiring mounts for the OPO top Shell With additional wiring for the SFI Faradays, having a mounting scheme to use the real-estate on the top of the OPO shell is useful.

Collimator Polarizer/Diode readouts After each fiber in the current VIP layout, a polarizer is used to clean the polarization, with a waveplate to rotate back to S-pol, and a diode to read the rejected light level. The polarizer and diode could be combined into a single mount, and the waveplate avoiding by using a vertically oriented polarizer.

4-port 1in beamsplitter mounts Ideally these should be adjustable, but vacuum compatible mounts that expose all 4 beamsplitter ports may be difficult to come by. We can either machine an adaptor similar to Thorlabs H45A. Alternatively, the in-progress layout of Fig. **??** is designed to work with fixed BS mounts such as Thorlabs' Polaris-B1S.

3 SQZ: Suspension Paths

Fig 1 Shows the two principle suspended squeezing paths as dashed-red and dashed-purple. The A:SQZFC path is the OPO to filter cavity path and the A:SQZIFO is the filter-cavity to interferometer path after separating the beams in SFI1. These paths should have active wavefront control where possible, as well as have sufficient Gouy phase separation for alignment control.

3.1 SQZ: Filter Cavity to OPOS

The telescope design between the squeezer and filter cavity is shown in figures 6 and Fig. 7. These figures show the telescope in "reverse", from the filter cavity to the VOPO platform. This orientation places the mode constraint on the left of the plot, propagating to the unconstrained mode leaving the platform. These should be inspected along with the HAM7 layout of Fig. 1. The latter figure zooms in to the mode between ZM2 and ZM1, to see the beam size. The features will be explained left-to-right, traveling from the filter cavity, and detailing the constraints on this design.

Telescope Features and Constraints First thing to notice is that the beam is 10mm ⌀at ZM3 from the filter cavity, even with the strong FC1-AR lens. If the FC1 lens were weaker, ZM3 would need an ROC to further focus the beam for the diameter to reduce to $<$ 5mm by ZM2. With the large beam diameter on ZM3, the AOI is too large to use a curved optic unless the beam is threaded through the HSTS suspension (see G1901432). This level of astigmatism sensitivity also generally excludes this optic from AWC. The chosen FC1-lens allows this optic to be flat, and therefor have a larger or more flexible AOI.

After ZM3 is a beam waist. ZM2 could be placed before or after this waist. It was chosen to be after so that the waist could be used for profiling and mode matching (see sec. 8). The additional distance also allows a smaller AOI on ZM2. The 532 and 1064 beams image to waists at different locations due to the 2% difference in index of the fused silica FC1 substrate.

Also noticeable is the Gouy separation of ZM3 and ZM2, which are guaranteed to be degenerate (0°, or 180°) for essentially any telescope design, since the beam is 10mm on ZM3 and

the baseline is much too short to accumulate any phase without placing the small waist on ZM2.

The beam diameter at ZM2 is chosen to be 5mm (w=2.5mm). This is flexible, and determines the distance from the waists and the ROC chosen for ZM2. The 5mm choice allows strong wavefront actuation, at the cost of some sensitivity to AOI from the optic curvature. The other alternative is a 4mm ⌀beam, which would require a ROC of $\approx 0.65m$, rather than 0.85m ($\approx$ 200mD difference).

The ROC of ZM2 is chosen to place the next waist on ZM1, for the Gouy phase separation needed by alignment control. Due to the short baseline, the waist on ZM1 is necessarily <1mm⌀. AWC and alignment control are not simultaneously possible on the FC path due to the baseline. The analysis of the ZM4-ZM6 path shows that it would be possible to get a beam diameter of 2mm on ZM1, but then only have 20°of separation with ZM2/ZM3, which is not acceptable for alignment control.

For these reasons, the 776um diameter waist is imaged on ZM1, which is chosen to be flat. This allows for the larger AOI that helps the tight VIP layout. The baseline between ZM1 and the VIP is as short as possible due to the rapidly diverging 532 FCGS beam. Keeping that beam small helps with FCGS mode matching and beam quality.

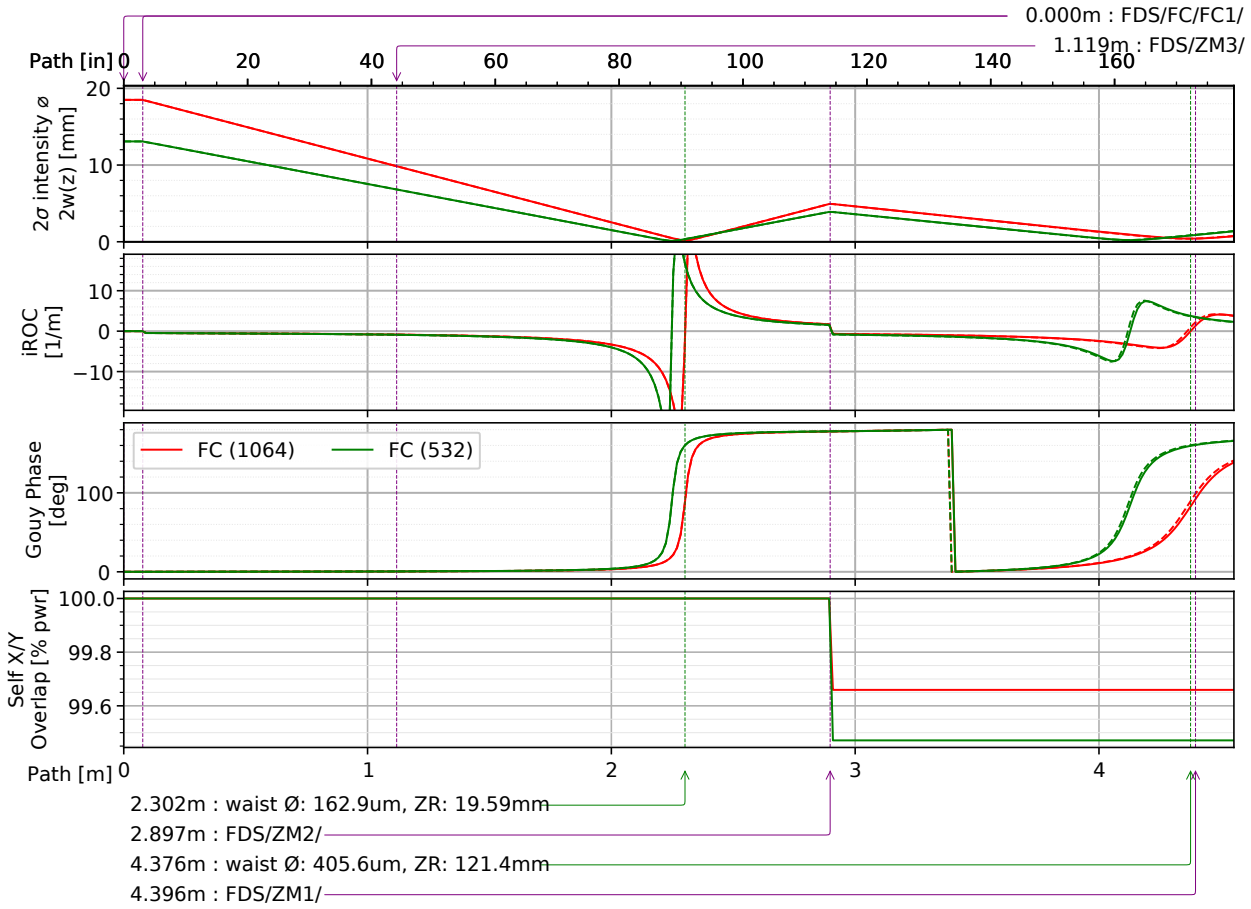

Figure 6: Telescope design between the OPO Platform and the filter cavity, shown as a beam propagation from the cavity towards the platform (ZM3 to ZM1). The waists given are for the 1064 SQZ field Y transverse beam parameter. The dashed lines show the X profile and effect of astigmatism from 3°modeled AOI on ZM2.

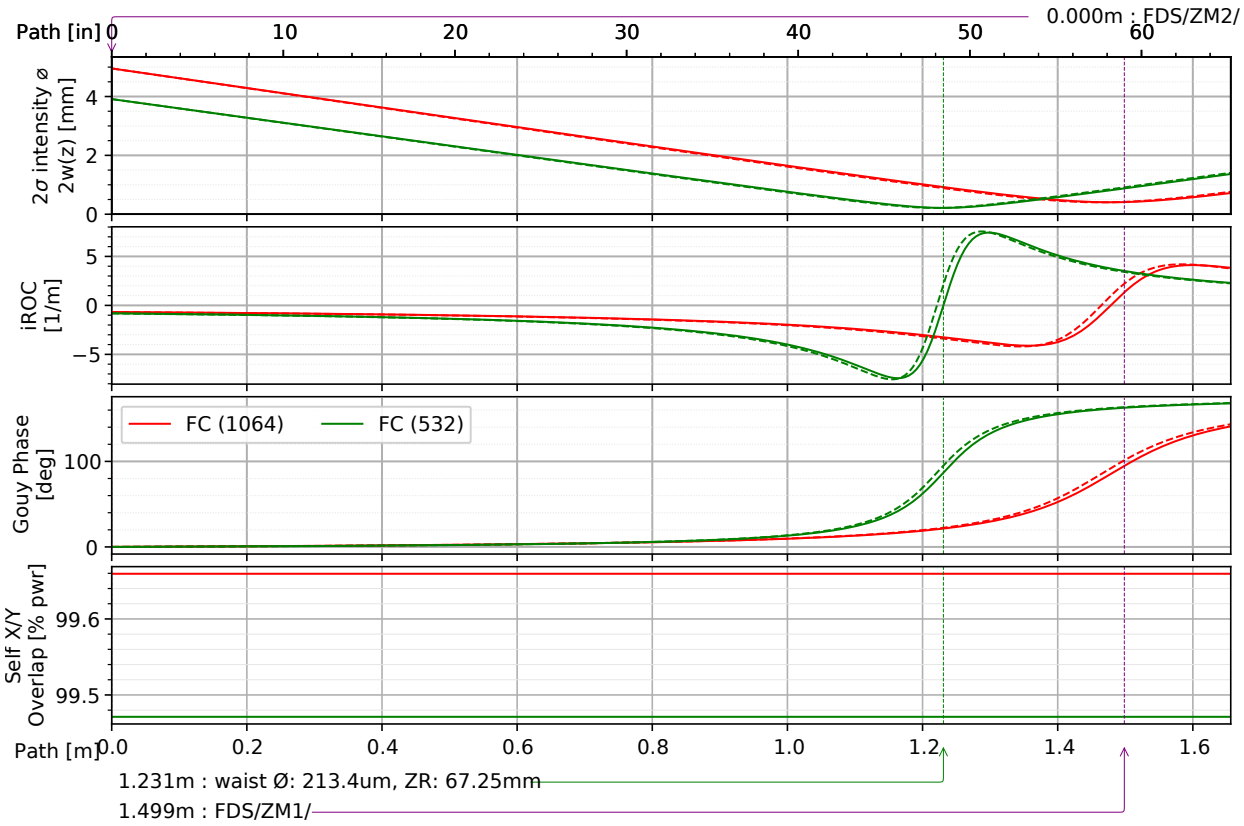

Figure 7: Zoom of fig. 6 between ZM2 and ZM1, to see the beam diameters. This plot shows the waist of the 532 Filter Cavity Green Sensing (FCGS) field, which is displaced from the 1064 waist due to differential lensing of the FC1 substrate and 1m AR-surface lens. The right-extent of the plot is the beam landing on the last mirror of the OPO platform (A:M3).

Placement and AWC Interfacing The only curved optic, which is also an AWC optic, is ZM2. It is in a path with a strongly diverging beam, and so is very sensitive to placement. Alternatively, it is very sensitive to curvature variations in the FC1-AR lens. The placement sensitivity allows the FC1 lensing variations to be compensated, and in this propagation direction, AWC controls the waist location W.R.T ZM1.

The AWC, when unidirectional, will likely be configured to increase the ROC of a concave lens (flexing the sagitta of the optic into the beam, decreasing concavity). If multiple optics are purchased, increasing the curvature is desirable, both to complement the actuation sign of AWC, but also since the alternative, smaller beam size, uses a smaller ROC. The chosen $0.85m$ ROC corresponds to $\frac{1}{2*0.85\text{m}} = 588\text{mD}$. Adding 40mD gives an optic with a ROC $0.80m$. At the far extreme is the 0.65m ROC needed for the 4mm diameter beam choice, which is 769mD, 200mD from the 0.85m optic.

The VIP will still include a translation stage of one lens (A:L2, see fig. 2 and sec. 4.1), which is intended to be on the filter cavity path. That translating lens will actuate both the beam size and location W.R.T. ZM1, and so will be somewhat degenerate with the ZM2-AWC, but will provide the orthogonal D.O.F of mode matching adjustment.

The figures in this section, fig. 8 and fig. 9, show plots of the beam mode as two degrees are scanned. The first figure shows the scan of the ZM2 actuator ±50mD from the nominal design along with the scan of the L2-translation stage. The left plot shows the effect on the mode at the FC1 HR surface and the nominal beam. The contours show the overlap with the nominal. The right shows the generation of LG1 mode from the mismatch. Since there is a different beam parameter in X and Y due to astigmatism, HG modes are more appropriate for the plot, but also more difficult to relate to loss without combining the X and Y plots, so the LG calculations are shown.

The second figure shows the effect of as-built variations on the mode-matching solution. A 1% variation in the FC1 S2 ROC can cause 10% mismatch. This implies the initial matching procedure will have to do better. On the other hand, comparing the LG1 generation of both plots shows that the ZM2 actuator is phased well to account for the positioning and curvature variations expected.

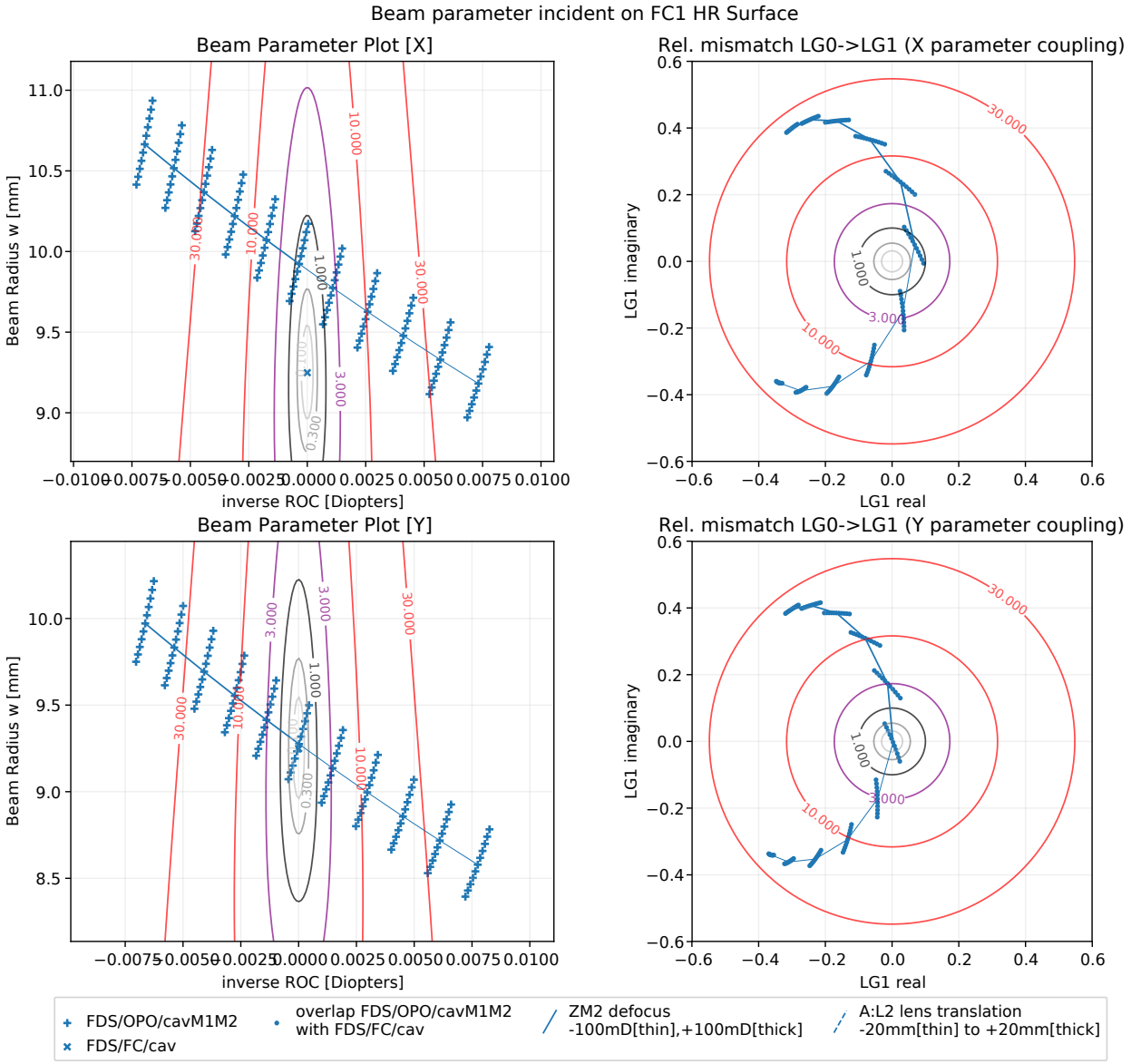

Figure 8: View of the wavefront actuation in beam parameter and LG1 couplings for the ZM2 and A:L2 translation stage.

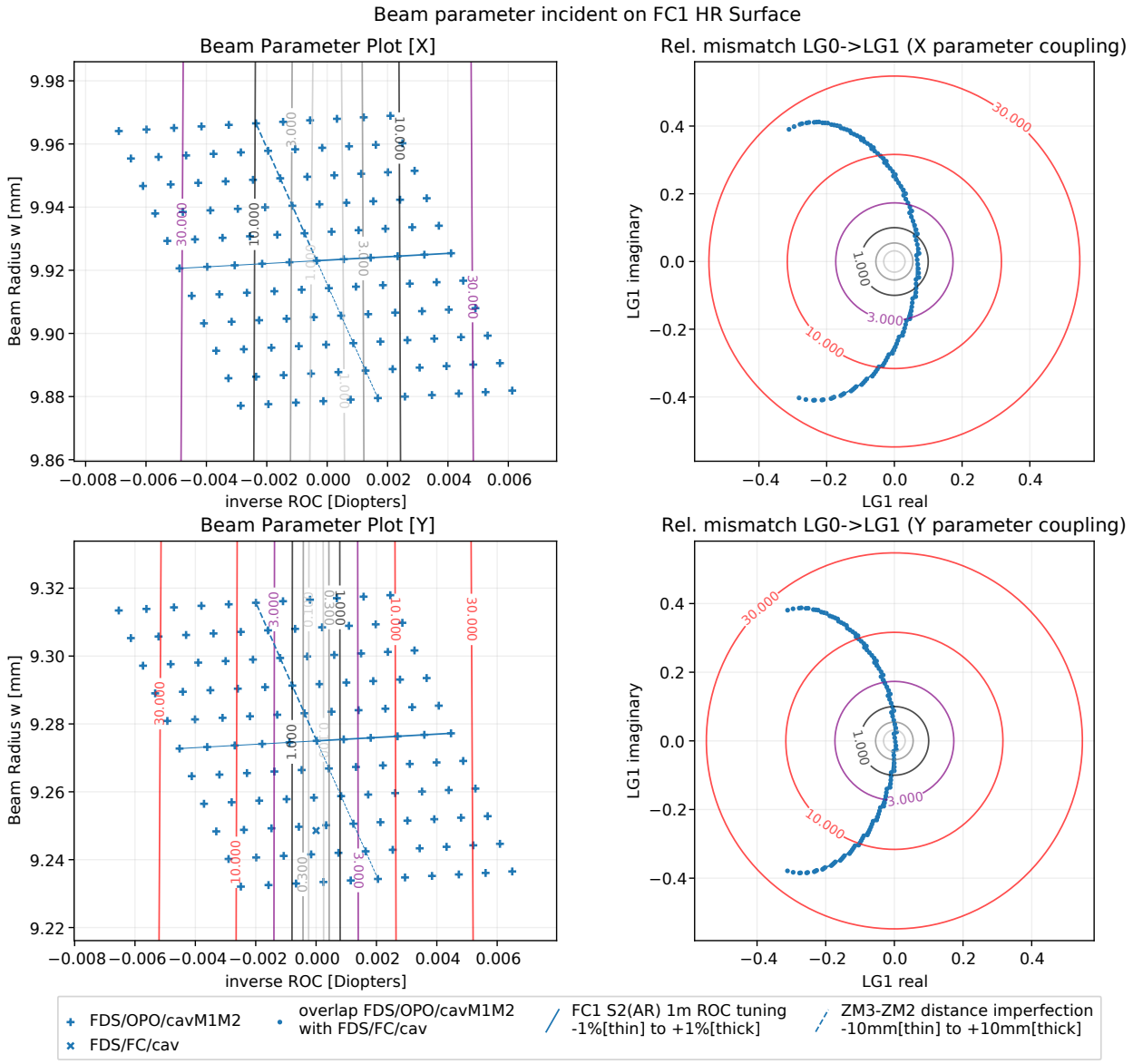

Figure 9: View of the wavefront variation from installation uncertainty in the FC1 AR surface lens and placement of ZM3 and ZM2. The two uncertainties are extremely degenerate, as seen in the LG1 coupling parameters.

3.2 SQZ: OPOS To SRM

The telescope between the OFI and ZMs 4-6, transporting the SQZIFO path from the VIP to the interferometer, is shown in Fig. 10. Similarly to the previous section, the plot is arrange with the fixed cavity mode of the interferometer on the left. This shows the sequence of constraints towards the arbitrary parameter leaving the VIP platform. Figure 11 shows the true propagation direction of the squeezing field.

Fig. 10 shows an assortment of beam parameters from the interferometer, due to modeling uncertainty. These parameters reflect the arm and SRC cavity modes using optics and lengths from Dan Brown's Finesse models and Anna Green's updates for LLO, which are written up in T1900159. These generally agree with the as-designed parameters given in T0900043. Additionally, the nominal output beam parameter from T1200410 assumed for the OM telescope design is plotted. The interferometer parameters are plotted as the arm mode propagated through the SR optics, as well as the circulating SRC mode.

For the actual telescope, the beam first transmits through the OFI, which has two 1in relay optics mounted (OFI/ZR1/ or ZR2 in the plots). Any desired beam adjustments on ZM6 and ZM5 require a lens to be installed between these relay optics. The given design does not include one, but following considerations may motivate at least a mounting hole be provide for the option in the future.

Assuming no lens on the OFI SQZ path, the beam encounters ZM6 approximately one Raleigh-range before the waist. ZM6 has a large AOI, and so cannot have curvature (see Fig. 30). Due to the propagation length from HAM5 to HAM7, and the desire for the beam to be large enough on ZM5 for AWC, the Gouy separation is 128°. While this is far from the ideal 90 deg it a degeneracy that will degrade the noise performance of SQZ ASC by 50% (see eq. 57 in sec. 3 of T1900144-v3).

Avoiding this and preserving AWC on ZM5 is likely not possible. An additional OFI lens can either place the waist at ZM6 or at ZM5. If at ZM6, the beam is extremely large at ZM5. If at ZM5, the beam size is too small for effective AWC. Since the beam is large at the OFI, collimating the beam won't accumulate a Gouy phase between the two suspensions which is any less degenerate. Fortunately, ZM6 is place as close to the waist as it is. The final alternative is to place a weak lens at the OFI and move the waist slightly closer to ZM6, decreasing the degeneracy and reasonably increasing the size on ZM5. The chosen design was to exclude such a lens for simplicity.

Given these choices, the beam is nearly 4mm ⌀on ZM5, which is appropriate for wavefront control. This optic uses a 3.4m ROC concave optic to refocus the beam. This ROC is chosen to keep the beam 2mm ⌀and 20°of Gouy phase on ZM4. The size allows AWC to still have some actuation power, and the Gouy phase will make the degeneracy between the AWC actuators approximately $\sin(2\cdot 20°) = 0.64$, $\cos(2\cdot 20°) = 0.76$. This gives that the range (in field LG1 actuation) of the ZM4 AWC is reduced by $0.65\cdot\frac{2mm}{4mm} = 32\%$ from the ZM5 AWC, which is 10% of the range of coupling efficiency in units of power. The ZM5 AWC will then have to consume $\frac{2mm}{4mm}\cdot 0.32 = 38\%$ of its range (in field) to compensate for the degeneracy. Given the design constraints to make strong AWC actuators, this seems acceptable.

Additionally, this allows the ZM4 mirror to be flat, and the beam arrives on (actually, leaves)

the VIP as a collimated beam, which is particularly easy to characterize with beam profiling.

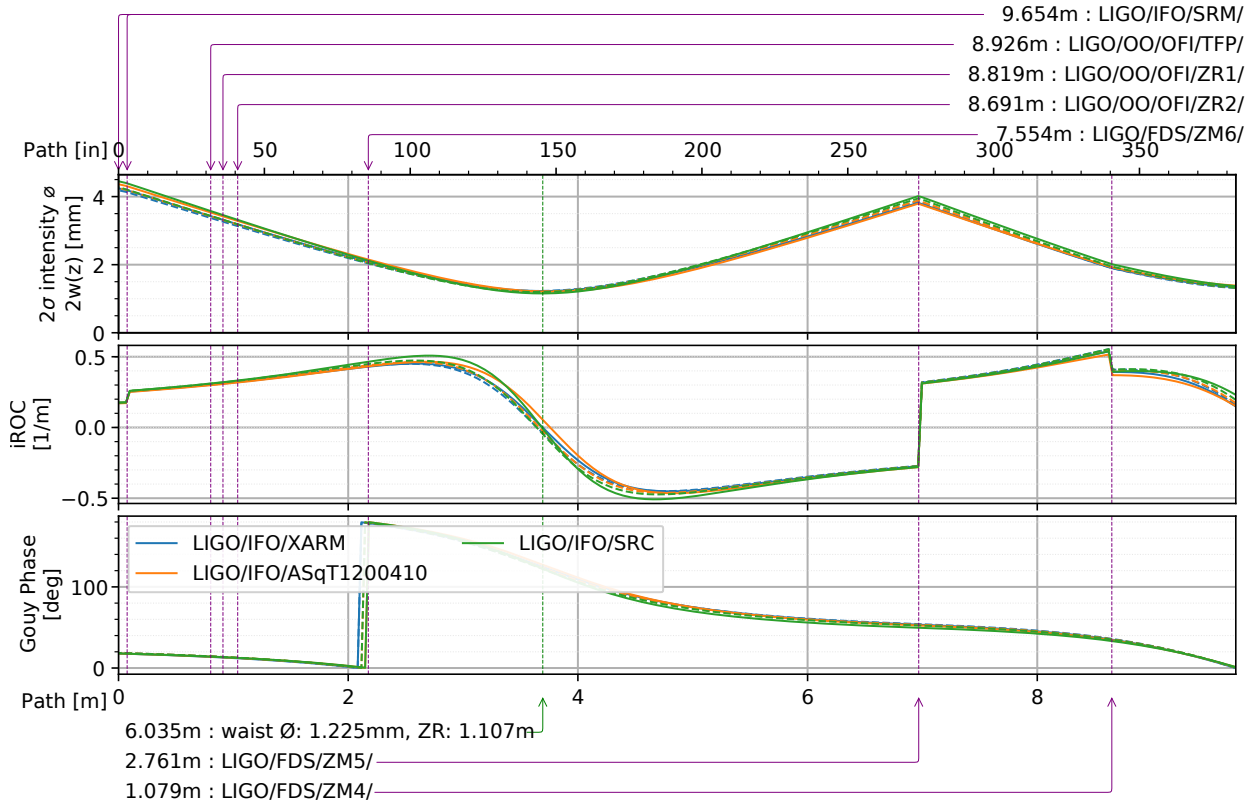

Figure 10: Telescope design between the OPO Platform and the Interferometer, shown as a virtual beam propagation from SRM towards the platform (ZM6 to ZM4). The waists given are for the 1064 ARM beam propagated through the SR cavity. The dashed lines show the X profile and any astigmatism.

Wavefront Control From the design above, the beam parameter on the SRM and OMC can be viewed in fig. 12. This figure agrees with the logic above. The range of the stronger actuation at ZM5 shows approximately 8% → 0% actuation range consistent with the 4mm beam diameter and choice of ±50mD actuation range for the plots $\left(\frac{kDw^2}{4}\right)^2 \approx 9\%$. For the ZM4 actuation, the range is approximately 2% → 0%, or $\frac{1}{4}$ of the ZM5 range. This agrees with the 2mm diameter beam that is half the size of the ZM5 actuator. Furthermore, the angle of the actuation in the LG1-space is nearly 45°, as expected from the Gouy phase separation.

The range of the weaker LG1 axis does not span the entire 10% mismatch envelope, but it is sufficiently wide that starting at 10% mismatch will allow one to land at 3% mismatch or better. Figs. 13 and 14 show how the addition of venting and static adjustments can further extend the range. While shifting the lengths doesn't help much, purchasing only 2 separate ROC's for the weaker actuator to double its range is sufficient to reach perfect matching from 10% after swapping the actuators , by going 10% to 3%, then swapping to go from 3% to 0% mismatch.

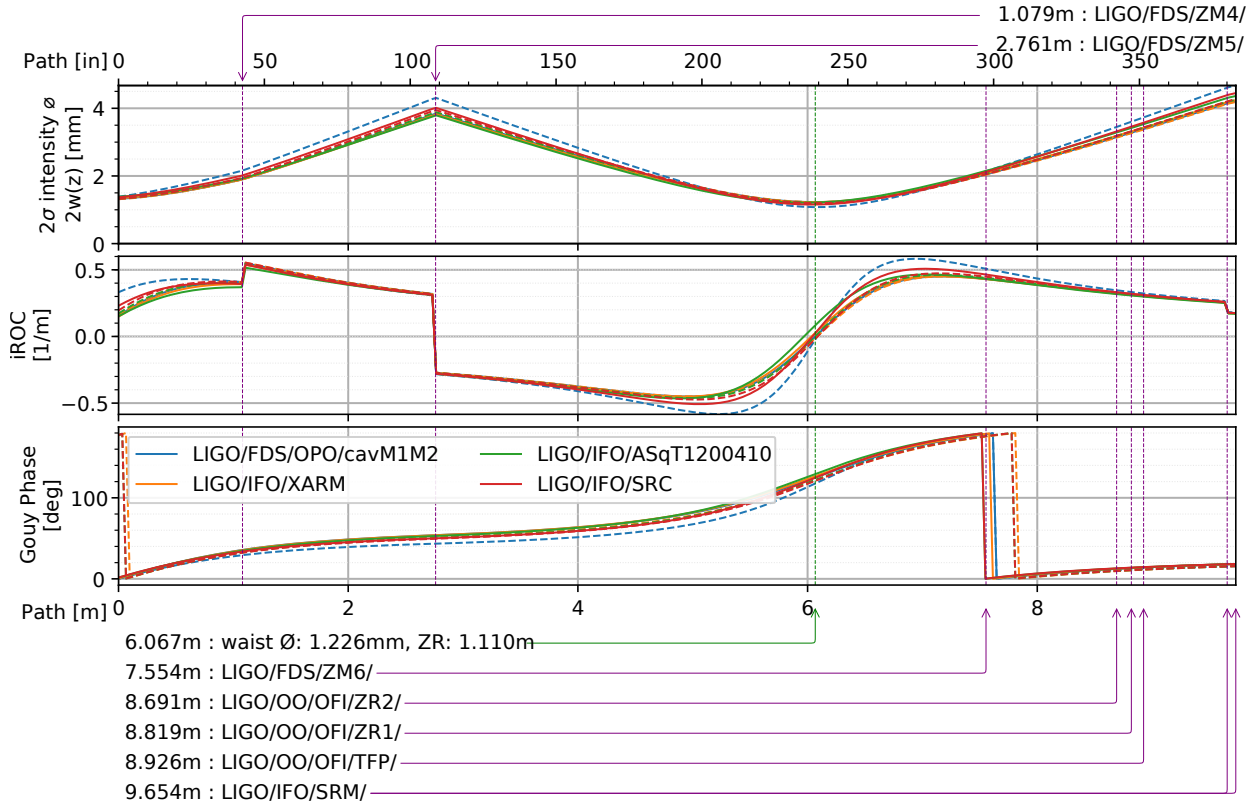

Figure 11: Telescope design between the OPO Platform and the Interferometer, shown as the true beam propagation from OPO platform towards the SRM (ZM4 to ZM6). The waists given are for the 1064 ARM beam propagated through the SR cavity. The dashed lines show the X profile and any astigmatism.

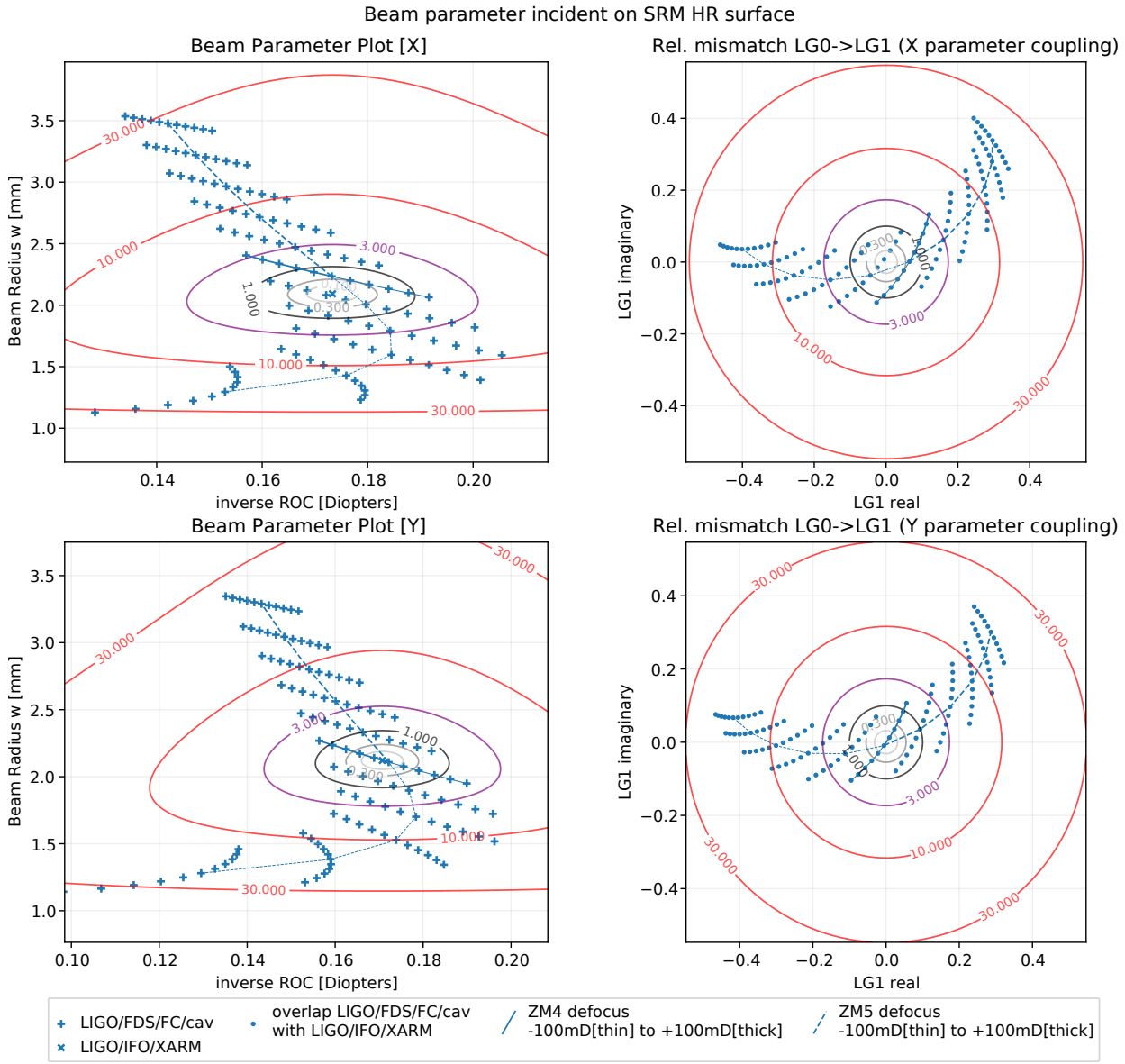

Figure 12: View of the wavefront actuation scanning ZM4 and ZM5. The right is plotted in the beam parameter at the SRM HR surface, to show matching to the nominal XARM mode of the interferometer.

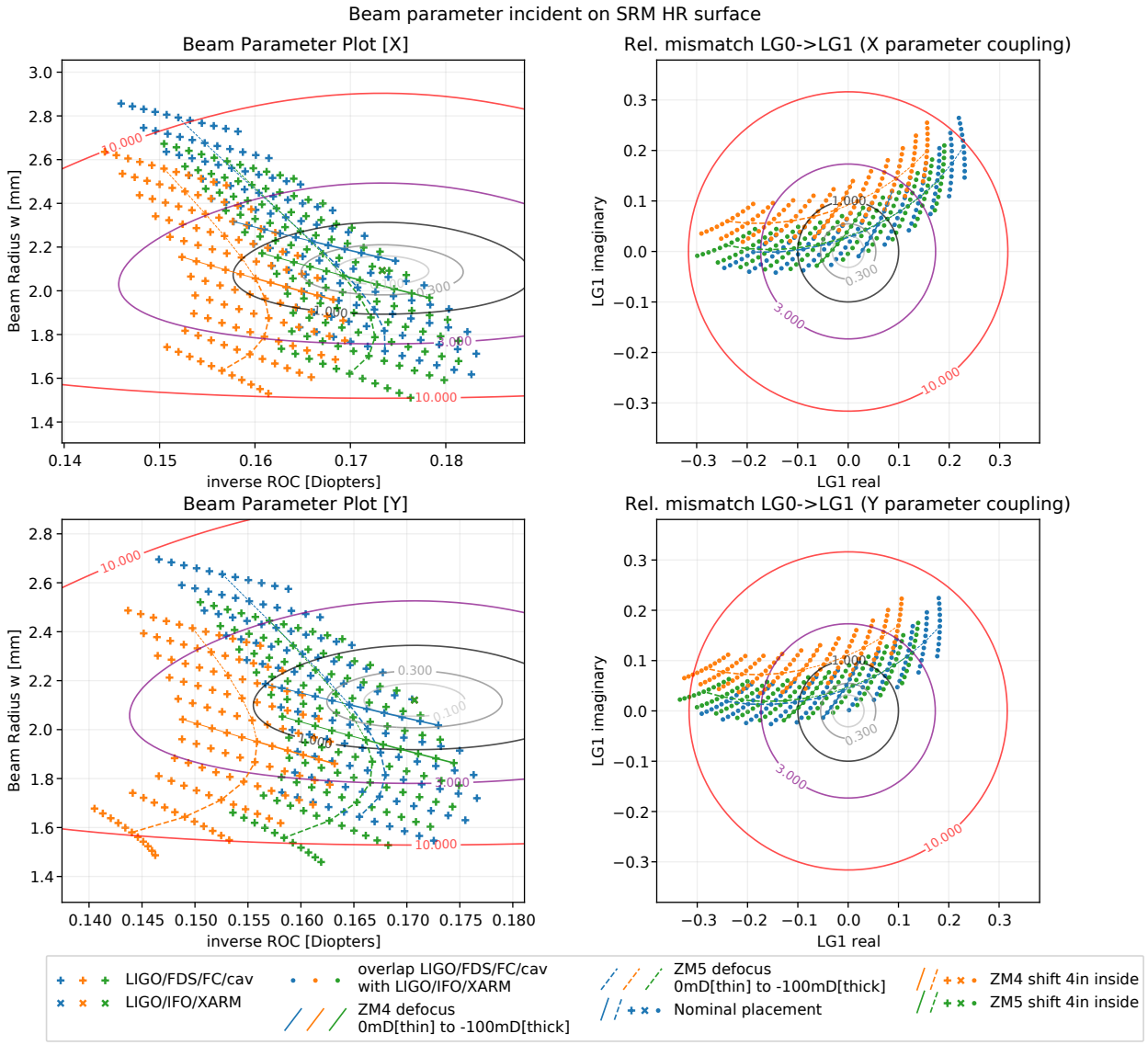

Figure 13: View of the wavefront actuation scanning ZM4 and ZM5. Additionally, mode-matching meshes are plotted with the ZM4 or ZM5 shifted inside by 4 inches. This shows the low sensitivity of the ZM4/ZM5 to placement, and correspondingly the inability to use placement to compensate for limited AWC range.

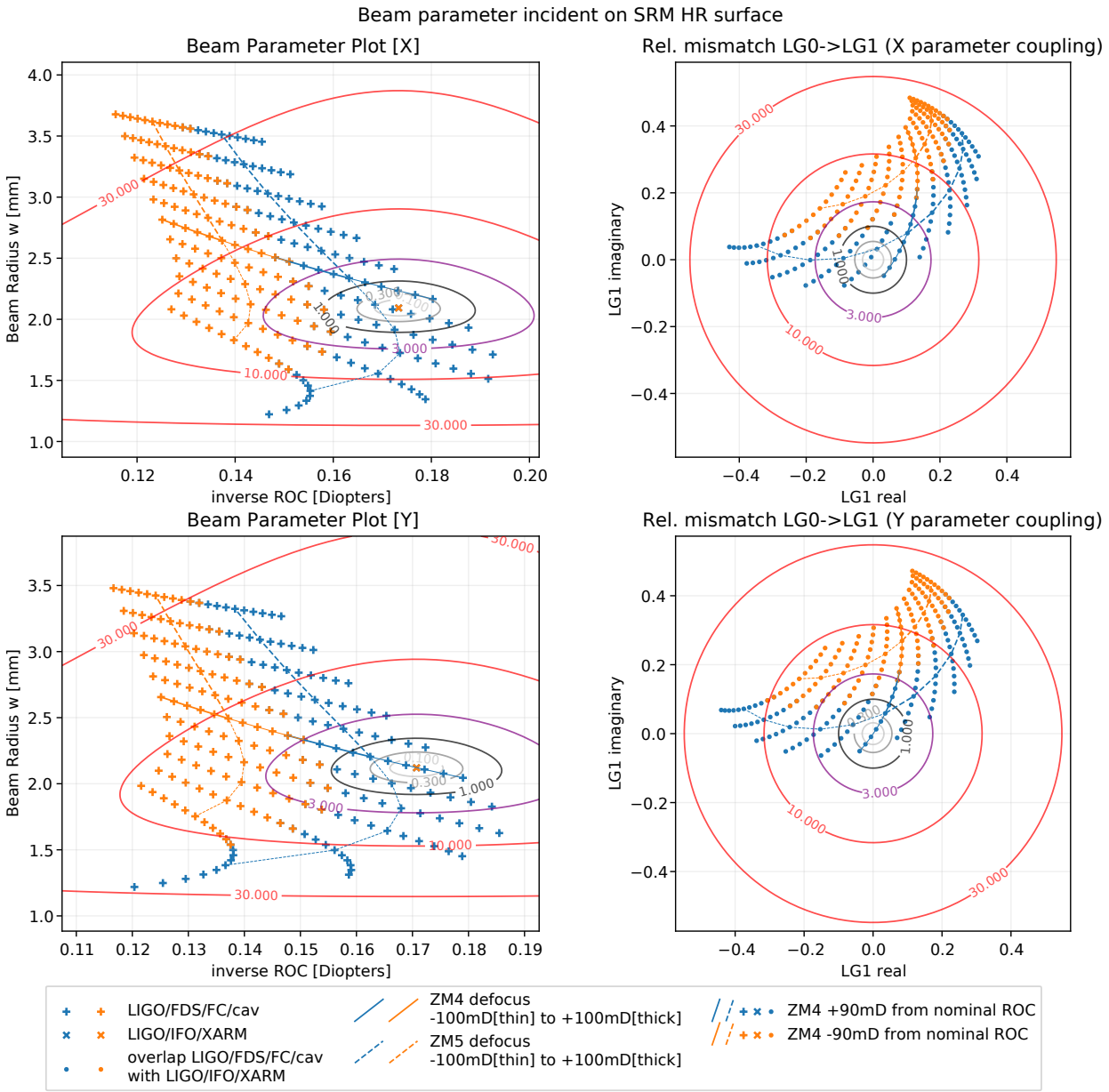

Figure 14: View of the ZM4, ZM5 wavefront control, where ZM4 is purchased in two ROC offset from nominal. This extends the effective range, allowing anywhere whithin 10% mode mismatch to be shifted to 3% without swapping ROC's and with the swap allowing anywhere in the 10% range to reach the ideal matching case.

4 SQZ: VIP and HAM7-ISI Paths

The designs of the suspended telescopes has some freedom in the mode on the VIP platform, but the OPO and two telescope paths must be coupled with a workable solution. Fig. **??** shows the two required paths, A:SQZFC (dashed red) is between the OPO and the filter cavity telescope (OPO to ZM1) and B:SQZIFO (dashed purple) is from the filter cavity to interferometer (ZM1 to ZM4).

4.1 SQZ: OPO to ZM1

This mode matching solution is for the Squeezing path to the filter cavity, matching the mode established by the ZM1-ZM3 telescope to/from the filter cavity. The mode from that telescope was "arbitrary", but ideally the telescope in this path can conveniently match to it, and is sufficiently adaptable that it may be adjusted to compensate for telescope variations within the limited space of the platform.

One additional issue with this path is that the SFI1 Faraday circulates the beam between the SQZFC and SQZIFO paths, and that couples the both the mode-matching solutions of those two paths, and any ability to measure and correct the beam on the SQZIFO path independently from the SQZFC path. While some coupling is unavoidable, the chosen solution should simplify initial setup of the lenses in the optics lab and hopefully minimize difficulty matching to the interferometer.

In this solution the first lens that (partially) collimates the beam into SFI1 does not need to move for static adjustments. Instead, two lenses, one weak and one strong, are used after the Faraday to provide an adjustability to the telescope. From exploring the solutions, the range of adjustments is limited, but well suited for the collimated beam as of ZM1. It is also possible to swap the two lenses (150mm and 350mm ROC's) for a single 100mm ROC, which has nearly the same total Diopters of focussing.

Fixing A:L1 will fix the optical mode on the SQZIFO path. For example, the SQZIFO telescope may be setup in the optics lab by placing a reflecting mirror at the waist of the SQZFC path (where ZM1 should be, 6.5in from the final optic, A:M3). With the retroreflection of the cavity simulated, the SQZIFO path can be setup. Then, in HAM7, the beam on the SQZIFO path will reflect the optics-lab measurements only once the beam is well-matched to the FC1 curvature. This will constrain 1 of the cavity matching D.O.F.s, it will not constrain the correct beam size on the optic, but that may be directly measured by beam profiling.

The matching solution is given in Fig. 15.

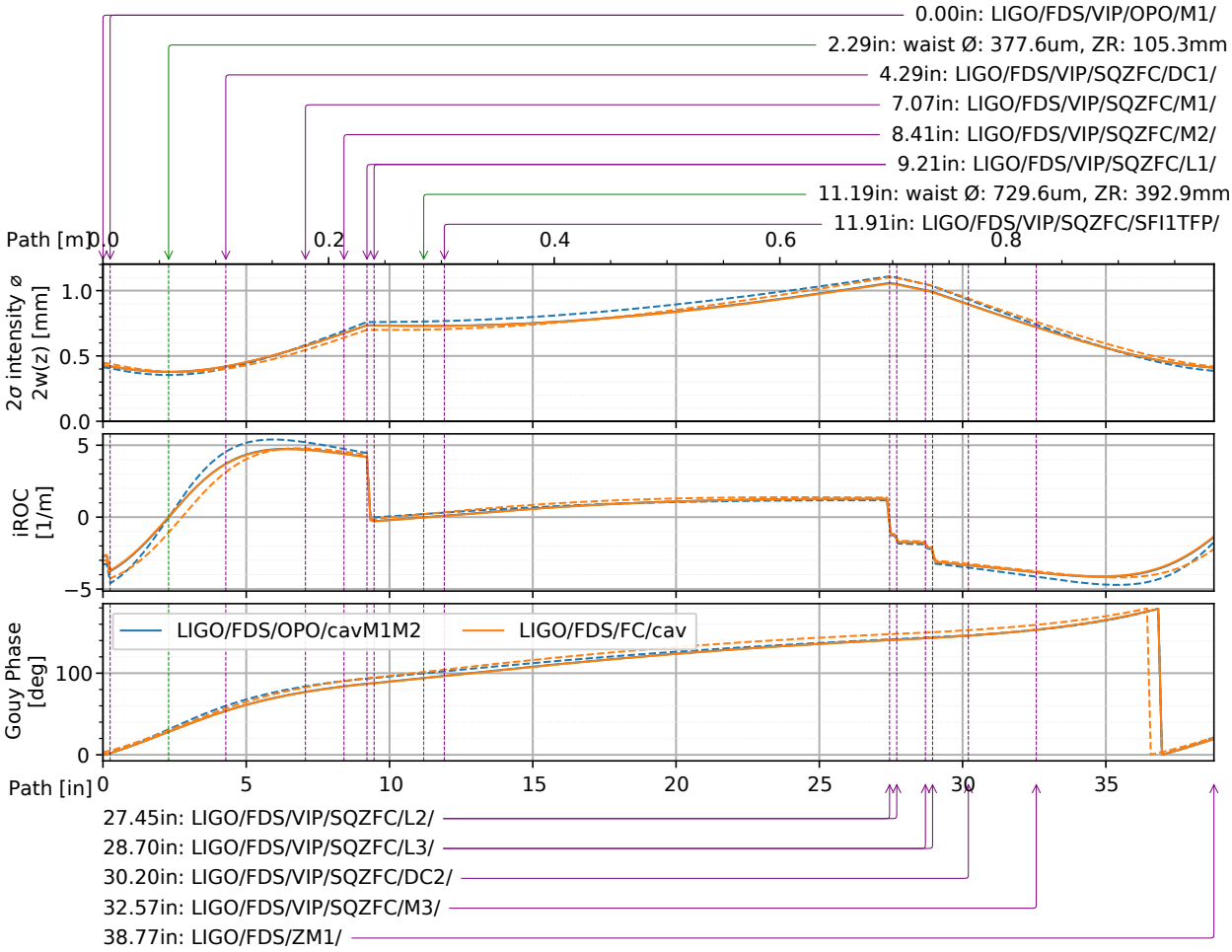

Figure 15: Mode matching solution for the squeeze path between the OPO and Filter cavity telescope. Here the OPO is propagating left-to-right and Filter Cavity mode right-to-left. the OPO astigmatism is partially matched to the cavity+telescope astigmatism. This solution is not (yet) computer optimized, but evaluates to 99.5% coupling efficiency.

4.2 SQZ: ZM1 to ZM4

Figure 16 shows the matching solution that transports the beam from ZM1 across the OPO platform to ZM4. The telescope shows ZM1 to the SF1 polarizer, but only after that polarizer is the telescope independent from the SQZFC path. A two lens solution is used to allow static adjustments of the mode without requiring changes to the ZM4-ZM6 telescope.

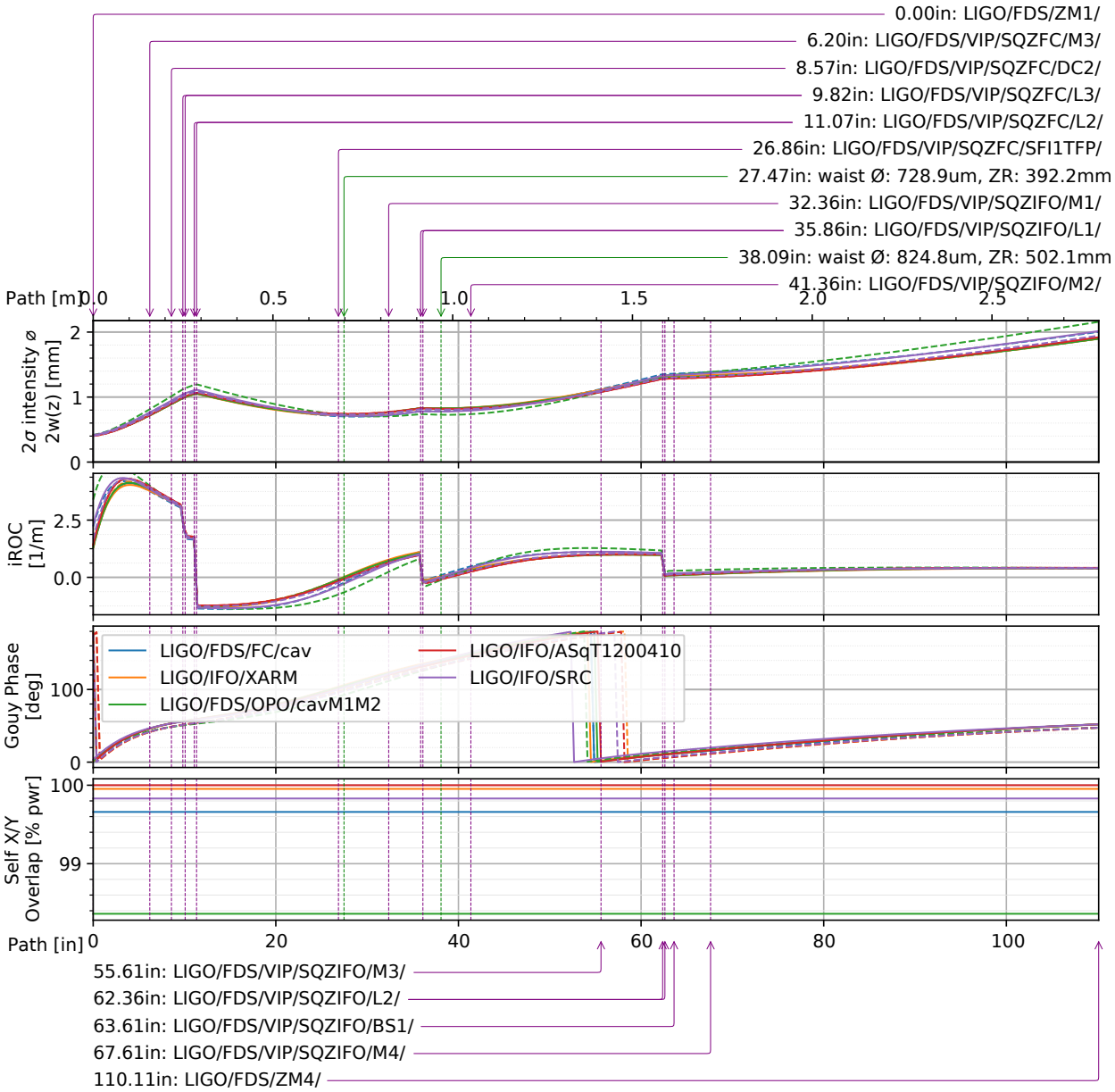

Figure 16: The mode matching solution between the filter cavity and interferometer telescopes, along the VIP platform. Only the SQZIFO indexed lenses should be adjusted for this path (those after the SFI1 thin film polarizer circulates the paths from SQZFC to SQZIFO). Refer to Fig. 2 to see the lens locations with respect to nearby obstructions. Each lens should have nearly ±1in of freedom.

4.3 SQZ: VIP to SQZ6 (Homodyne) path

This path just shows the pickoff of the SQZ beam to SQZT7 for readout by the homodyne. A 500mm lens is included to re-collimate the beam. This isn't strictly necessary, but the beam will be similar in size as on ZM5 (4mm ⌀) if it is not added.

One change from O3 is that the beam diverter is before ZM4 (ZM1 in O3), so alignment to the interferometer will not disturb the matching to the homodyne.

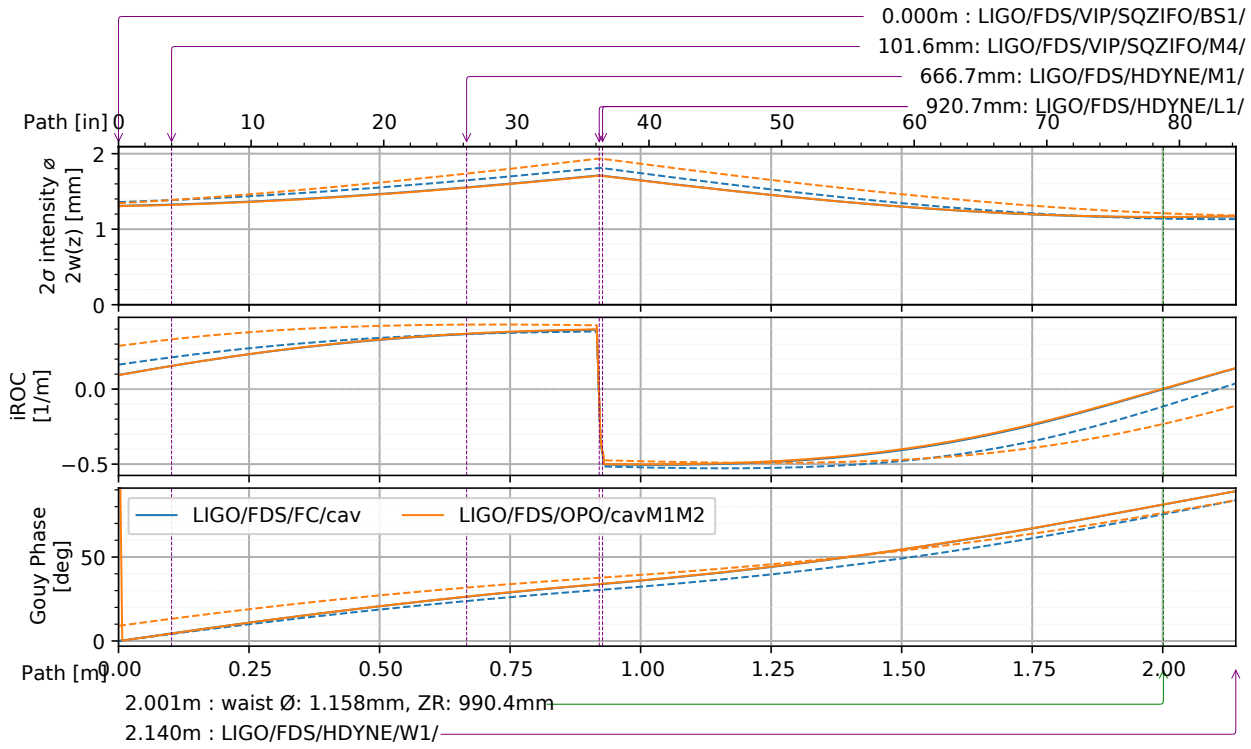

Figure 17:

4.4 SQZ: VIP to WFS path

This path shows the 1% pickoff beam towards wavefront sensors. A single lens reimages to a waist between the QPDs for Gouy separation. The beam sizes on the QPDs is similar to designs in T1000247 and T1300960. The signals showing in these WFS will also appear in the AS-port WFS. The OMC A and OMC DC QPDs could also be used and would avoid the 1% loss from this pickoff. The O4 design adds the pickoff for particularly clean and independent sensing, as well as improved shot-noise limited sensitivity as compared to alternative already-available QPDs. These WFS QPDs may also provide a clean length-sensing signal for the filter cavity as a backup from the OMCPD-derived length sensing signal.

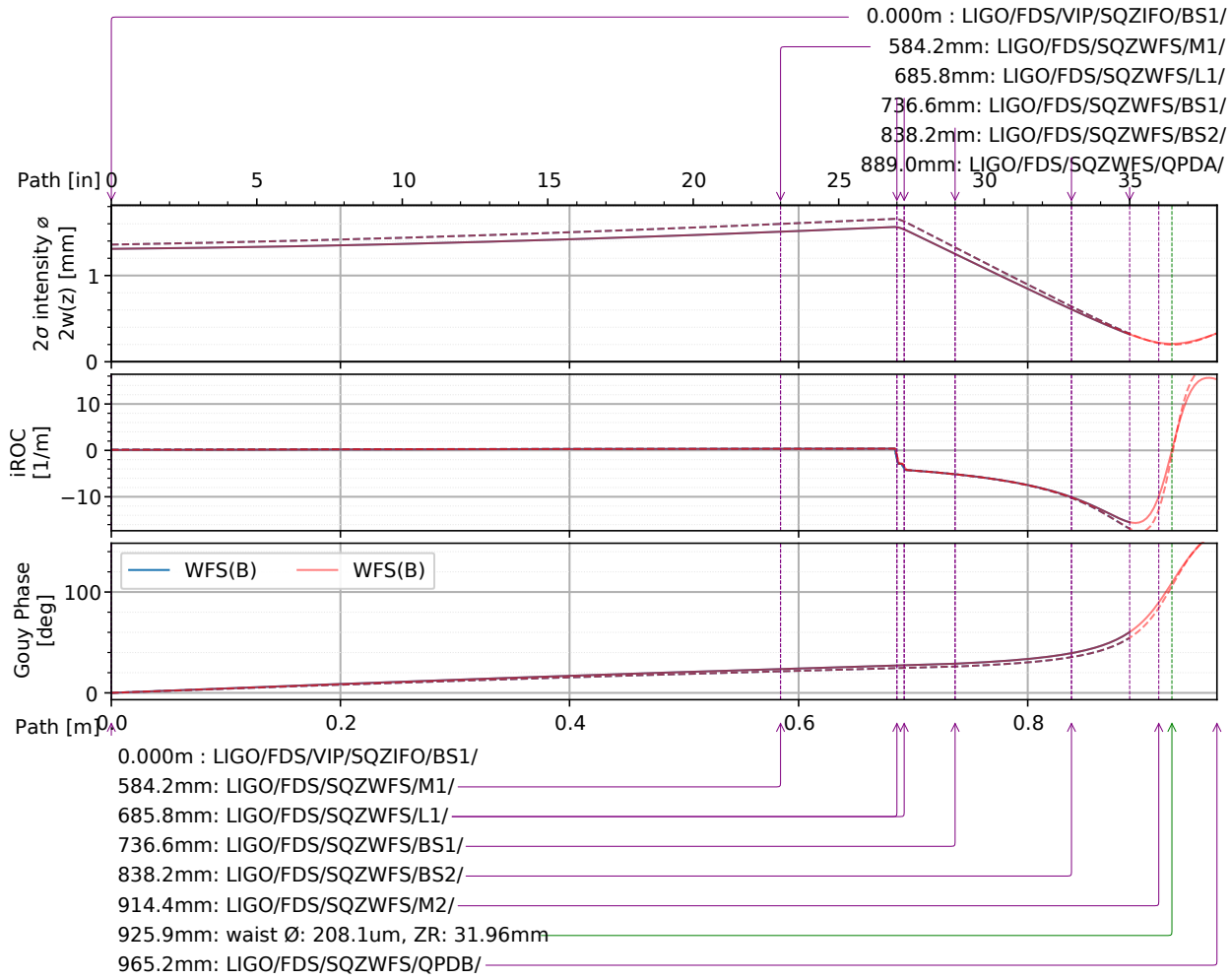

Figure 18: WFS Gouy phase telescope for independent ASC sensing. The blue telescope ends at SQZWFS/QPDA and the red at QPDB. The two QPDs are 1 Raleigh-range from the imaged waist.

4.5 SQZ: Inspection/Insertion path

This path is a non-essential auxilliary path for diagnostics, but potentially quite useful to reserve the space and components for, if not the time to set it up. A particular application for it is to see the residual beam that has pass through the OFI, SFI2 and SFI1. Sensing RF9, RF45, or the beatnote with the squeezer's RF3.125 will indicate the level of backscatter incident on the filter cavity.

This path may also be used for optical injections into the interferometer. The outgoing squeezer RF signals will provide a reference mode to match an injected beam to the interferometer telescopes.

To use this path, ZM1 must be deflected 3.5 mrad in yaw to hit SQZINS:M1. A 500mm lens is used to shrink the beam towards SQZT7. A 500mm lens is used to refocus the beam towards SQZT7. 2in optics may be more desirable if this path ends up useful, but would require a deflection near the limits of an HTTS range (7mrad).

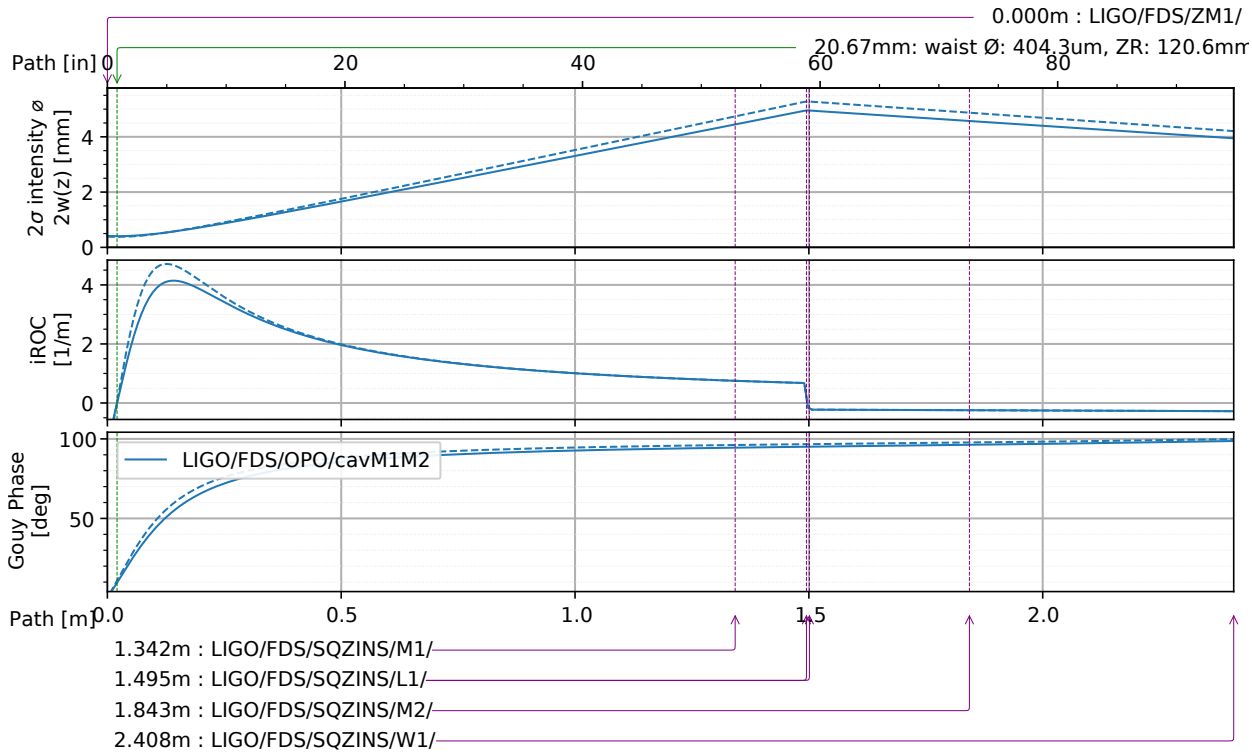

Figure 19: The insertion/injection auxiliary path for the squeezed light. This matching simply shows the large beamsize

5 Auxiliary Field Paths

The auxilliary fields on Fig. 1 and 2 include the CLF, pump and FCGS paths.

5.1 Pump paths

The pump path is altered from O3, and the 532 fiber collimators are assumed to output proper modes. Figure 20 shows the nominal matching solution. There are a number of additional solutions, particularly if the adjustability of the collimator is used to output a controlled but non-collimated mode.

Collimator to OPO

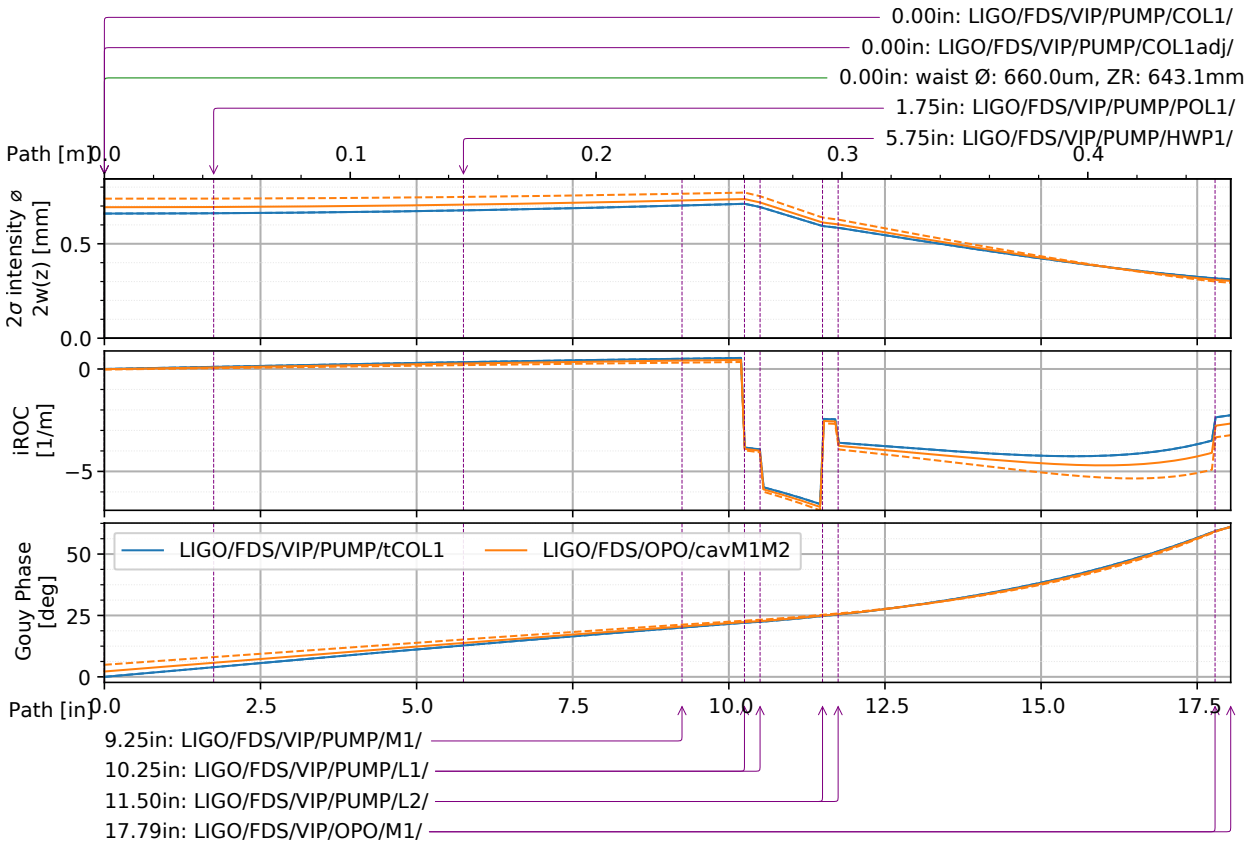

Figure 20: Matching solution between the 532 pump in-vacuum fiber collimator and the OPO.

OPO REFL to SQZT7

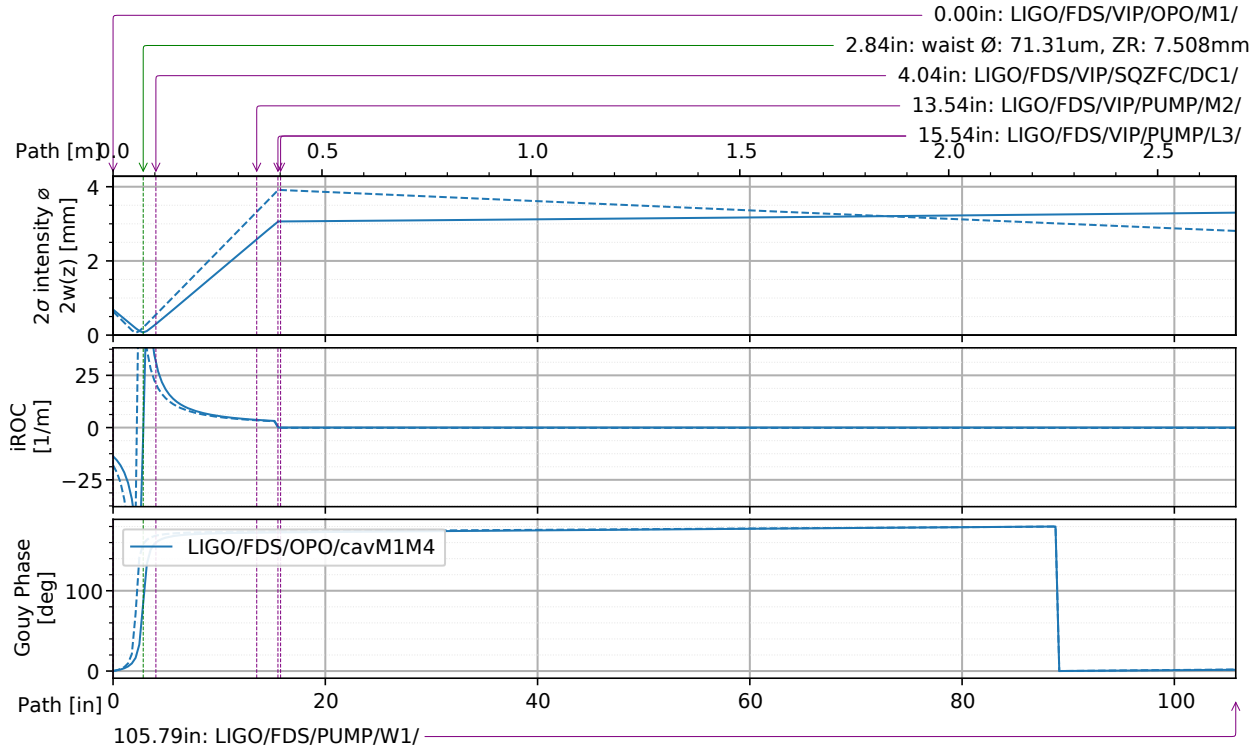

Figure 21: REFL path of the OPO pump to SQZT7.

5.2 CLF paths

The pump path is essentially the same as the O3 design, although the 1064 fiber collimators are assumed to slightly better collimated modes. Figure 22 shows the nominal matching solution. The existing solution may also be used if the collimator is adjusted to reflect the current output mode.

Collimator to OPO

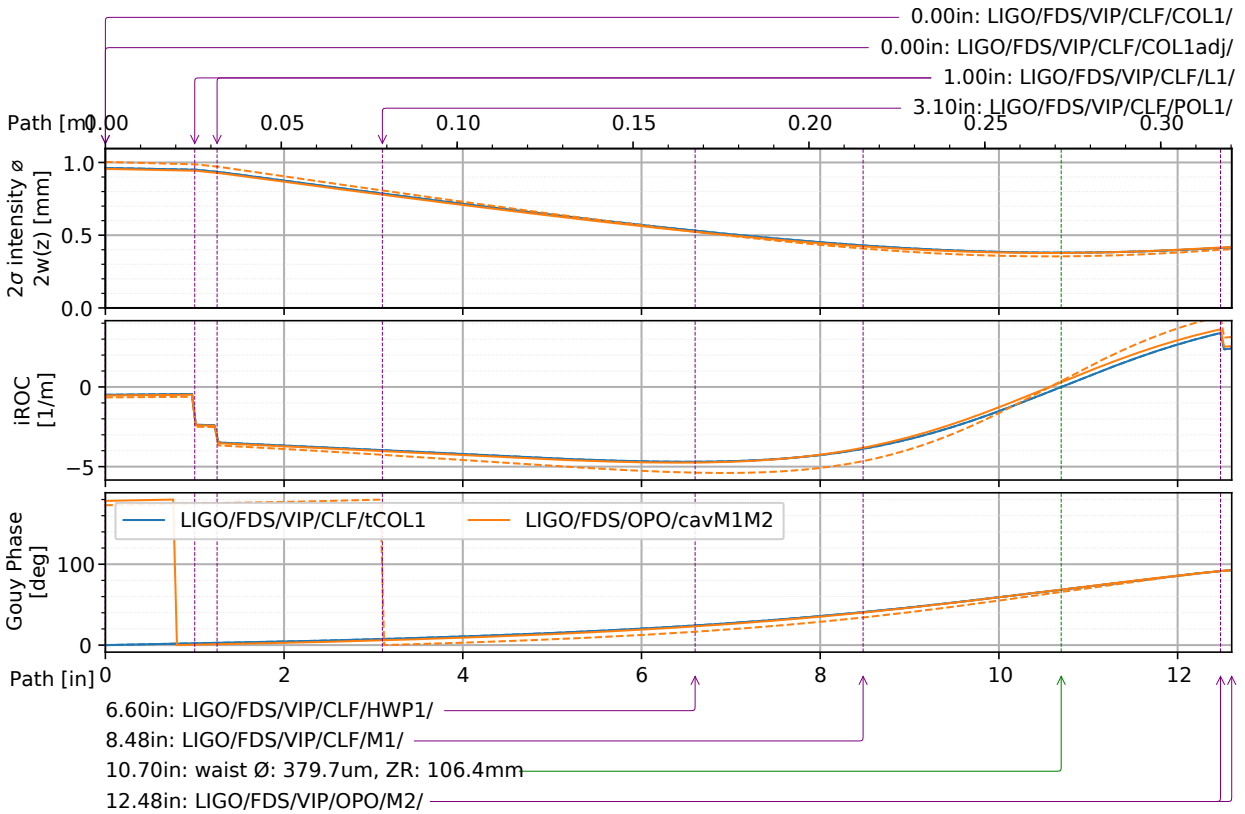

Figure 22: Matching solution between the 1064 CLF in-vacuum fiber collimator and the OPO into M2.

OPO CLF refl to SQZT6 (also OPO PUMP transmission)

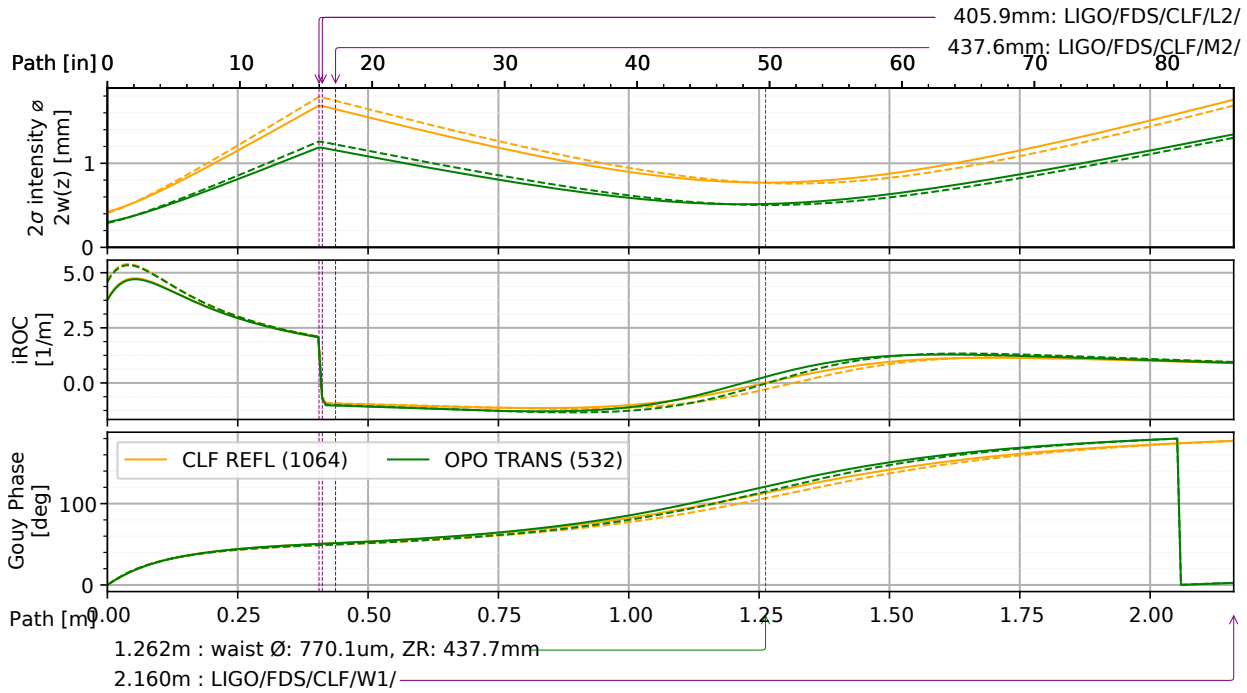

Figure 23: REFL path of the CLF. There is no space on the VIP for a re-collimating lens, so it is included on HAM7 immediately before the steering optic towards the viewport. The CLF REFL path also carries the PUMP transmission so both are shown.

5.3 Filter Cavity Green Sensing (FCGS) paths

The FCGS path is shown in fig 24 with the telescope on the VIP platform matching the beam in the ZM1-ZM3 telescope. Unfortunately, the matching solution currently does not put great Gouy phase between the FCGS:M2 and FCGS:M3 mirrors which will be picomotor actuated.

Collimator to SQZ towards Filter Cavity

FC REFL split to SQZT7 This path shows the beamsplitter that extracts the FCGS cavity REFL to send for readout on SQZT7.

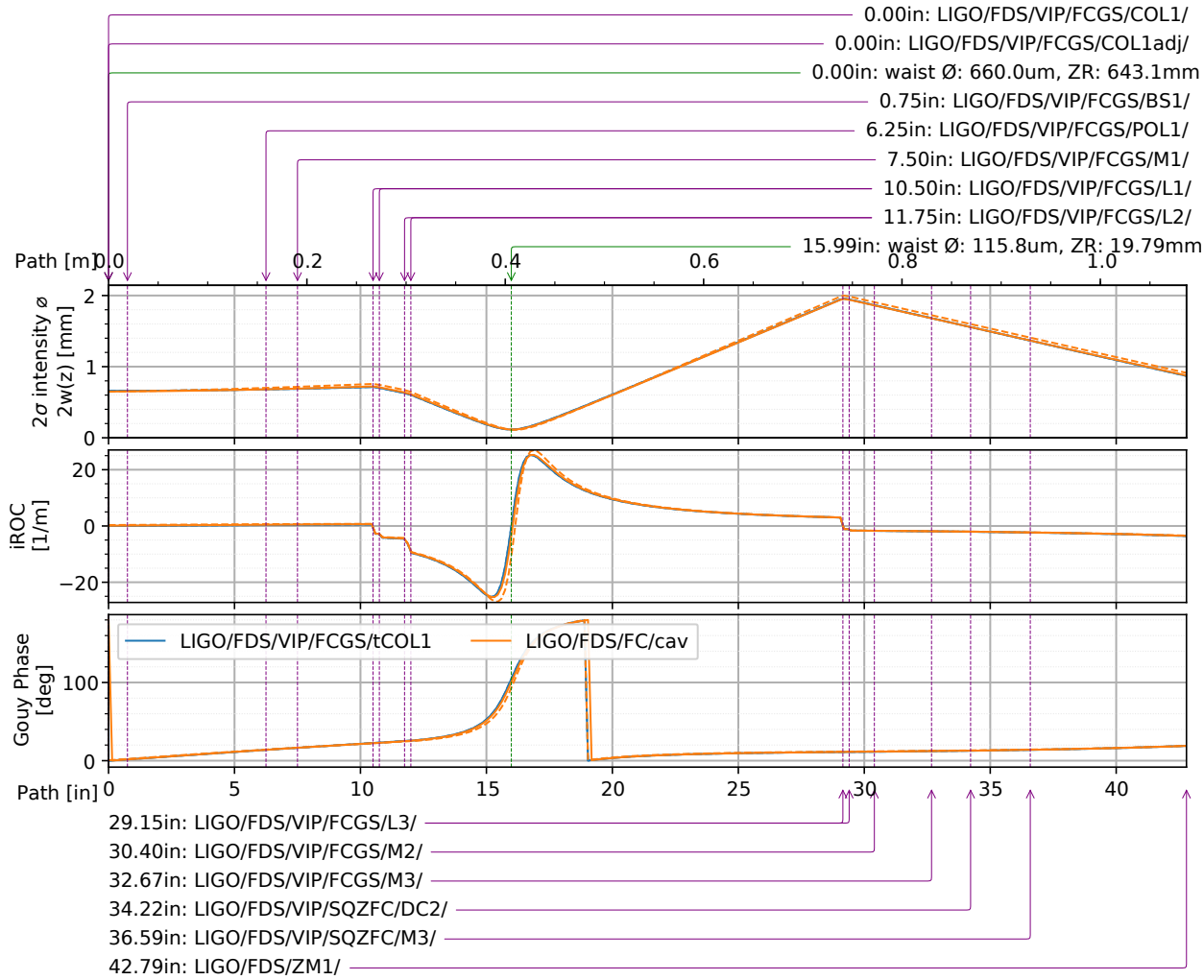

Figure 24: Matching telescope between the in-vacuum 532 collimator and filter cavity telescope. SQZFC/DC2 is the dichroic where the FCGS beam is stacked on the SQZ beam.

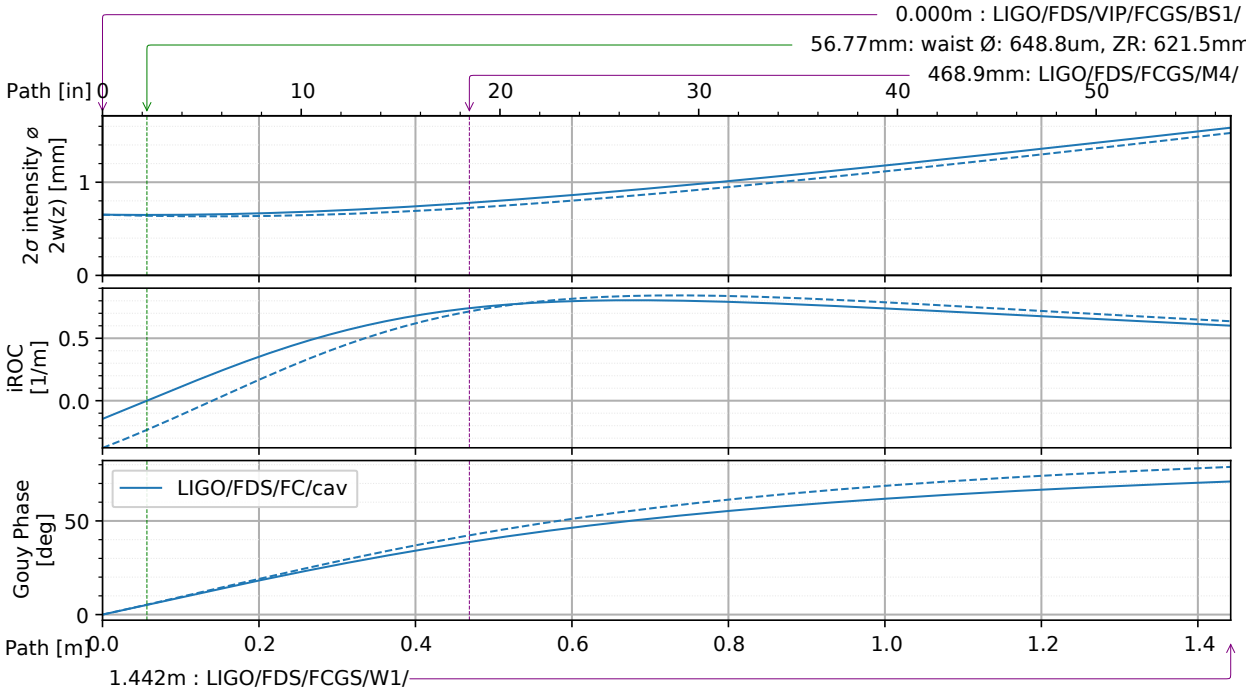

Figure 25: beam propagation of the FCGS beam from its REFL pickoff to the SQZT7 window. The mode is essentially the same as is output from the fiber collimator (when well-match to the cavity).

6 Transmission (HAM8) Paths

The HAM8 mode matching plots below should be viewed along with the layout of Fig. 4.

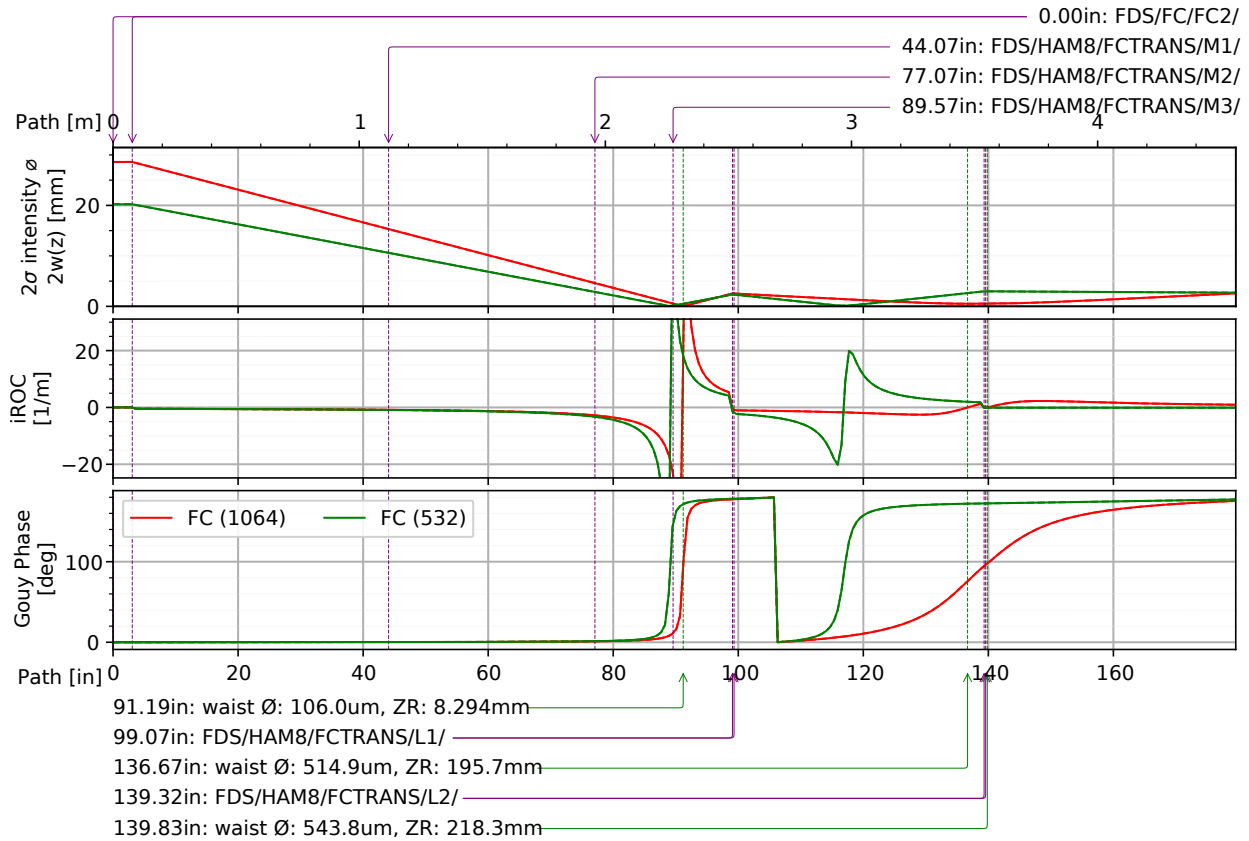

Figure 26: Transmission beam directly out of cavity. The 1064 beam is shown fully, the 532 FCGS is shown until the point it intersects with the dichoroic to split it off

Out Of Cavity

Figure 27: The 1064 beams on the transmission QPD paths. This path is showing only after the in-vacuum dichoroic.

To SQZ-Trans WFS

To HAM8 in-air table SQZT9

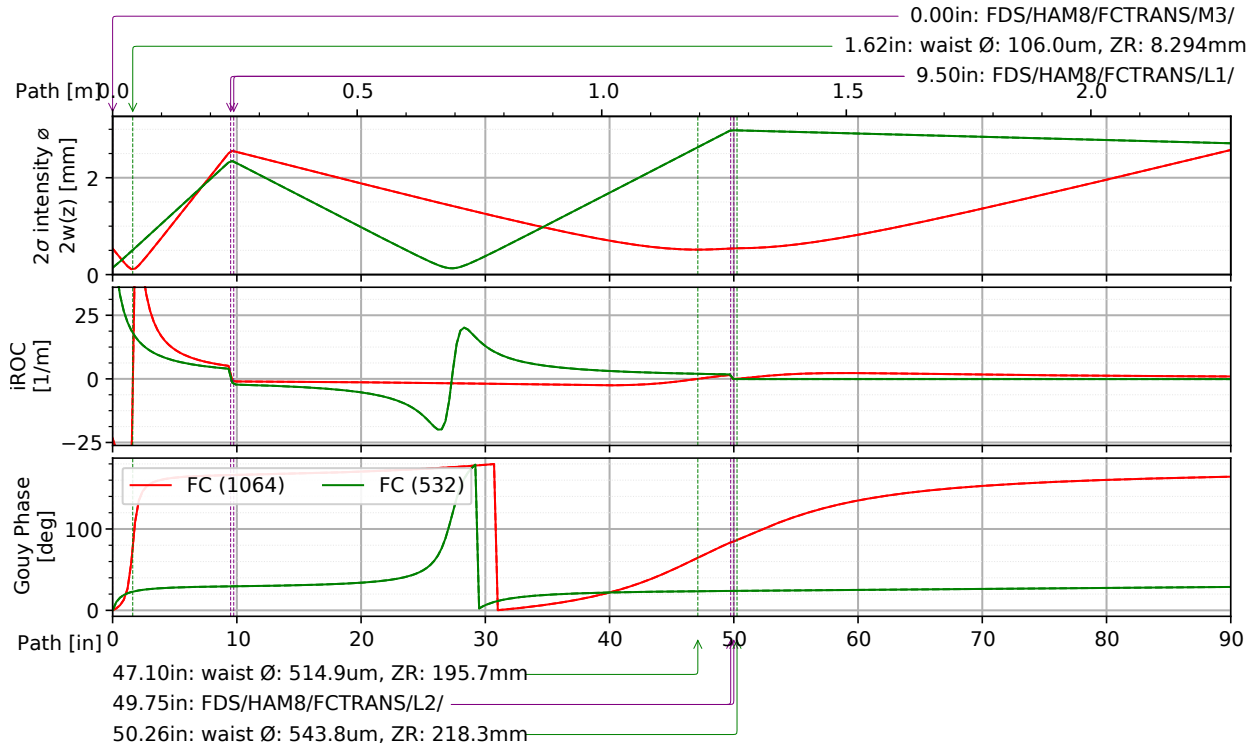

Figure 28: The 1064 beam after the dichroic on the path out of the HAM8 transmission window. This shows that the beam remains acceptably small. The waist is located on HAM8 to be profiled in the chamber so that the cavity telescope may be built on reflection from the FC2 optic using an in-air fiber-fed beam.

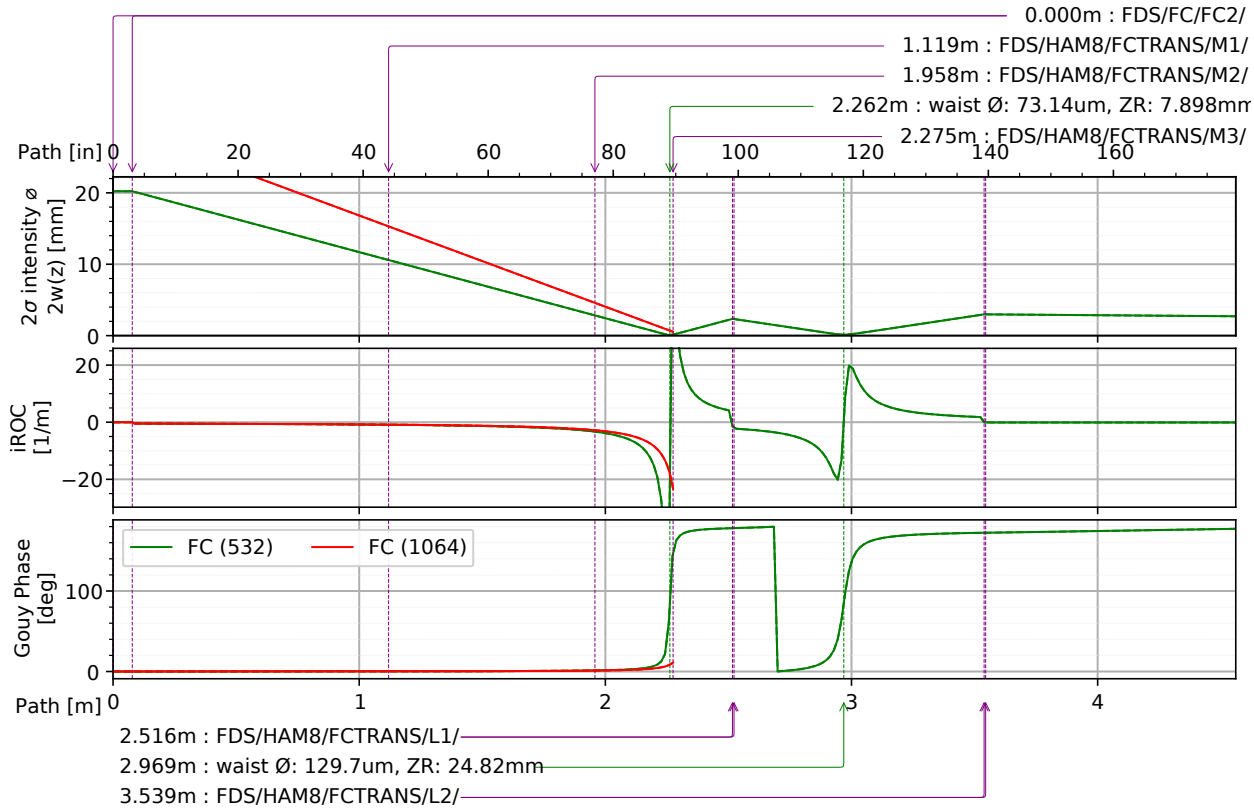

Figure 29: The 532 beam transmission to the HAM8 window. This beam uses a separate optic to collimate, and so may be difficult to get perfect without a reference beam. Ideally, the small transmission of 532 through a misaligned cavity should allow this to be established.

7 Initial Alignment Procedure

To obtain initial alignment, a 532 or 1064 beam, sufficiently mode-matched must be established, and the FC1 optic must be in-place. The ZM1-3 are then tuned to center the beam on FC1, as established through a beam profile on transmission of FC1. The ZM's are then tuned to maintain that FC1 centering, while aligning the beam down the 300m tube. Once the beam is found, in HAM8, the FC1 retro-reflection is observed, and FC1 is adjusted to align it to the incoming beam, this aligns FC1. Due to the strong FC1 AR lens, this will require iteration, as moving FC1 will change the deflection of the beam down the FC tube.

FC2 is aligned by reflecting back to ZM1

8 Initial Matching Procedure

8.1 FC1

The filter cavity initial mode matching will requirement an iterative procedure to converge to high static matching between the OPO and filter cavity. This will proceed in rough (0-90% MM), fine (90-96% MM), and AWC (96-100%) stages. The rough stage should be entirely in-air, the fine requirement vents, but ideally very few, and then wavefront control removes the residual static mismatch.

A principle issue with the filter cavity is the strong AR lenses on the optics and the precise placement of the ZMs due to the short and strong telescope between ZM2-ZM3. Inability to precisely place the suspensions, as well as substrate and polishing tolerances will require some measurement of the initial matching, without establishing a cavity.

Retroreflection overlap technique To get the beam approximately matched, the forward and retroreflecting beam from FC1 can be sent through an iris. The iris is placed between 3db clipping points on the waist between ZM2-ZM3. A class-B 50/50 BS-cube and mount can then be added on the ZM1-ZM2 path (where the beam is nearly collimated, and the small path-length change is unimportant). The splitter allows one to measure the power loss of the retroreflection through the iris. ZM3 is then moved to adjust the waist position of the retro beam from FC1. The 3db points from ZM3 translation can be measured and ZM3 may be placed between them.

This technique was used in LASTI for the 16m filter cavity and managed 90% on first attempt using only a beam card to establish waist position, rather than clipping measurements through an iris. The LASTI FC telescope was similarly sensitive.

This technique constrains the wavefront curvature to be flush with the FC1 HR surface (flat), as that will cause the forward and reverse beams to overlap. With beam size measurements at FC1, the matching should be well-constrained.

Future versions of this document will analyze the sensitivity with mode-matching plots.

Profiling Technique A class-B 2in optic is used to scroll the beam through a photodiode or beam profiler. This is used since the beam is too large for profiler CCDs, and the deflection/screw adjustment can be known for the optic mount. The beam width is measured this way at FC1 and at FC2. The 300m baseline will strongly constrain the matching for FC2 if the beam size is correct after such a propagation distance.

8.2 FC2

The transmission signals of the filter cavity will also require a procedure for establishing the initial mode matching. Since the cavity can not be operated in air, and the transmission power is extremely weak otherwise, a beam must be injected to establish the initial alignment and mode matching. The retroreflection techniques above will be used to establish the sensitive position of the lens I:L1.

The injected transmission beam will be profiled in-chamber to ensure that it is an expected mode and waist position. For course adjustment, I:L1 will be shifted until the reflection overlaps the incoming beam. The QPD paths are arranged then for convenient beam profiling along the arm to I:QPDB. The lens can then be shifted until the waist is properly located between the QPDS.

The same will be done for the 532 FCGS transmission beam, although a separate 532 source must be available. The 1064 source will be delivered by fiber to HAM8, and the same telescope used for transmission injections is to be used for initial telescope setup.

A Additional Wavefront actuation plots

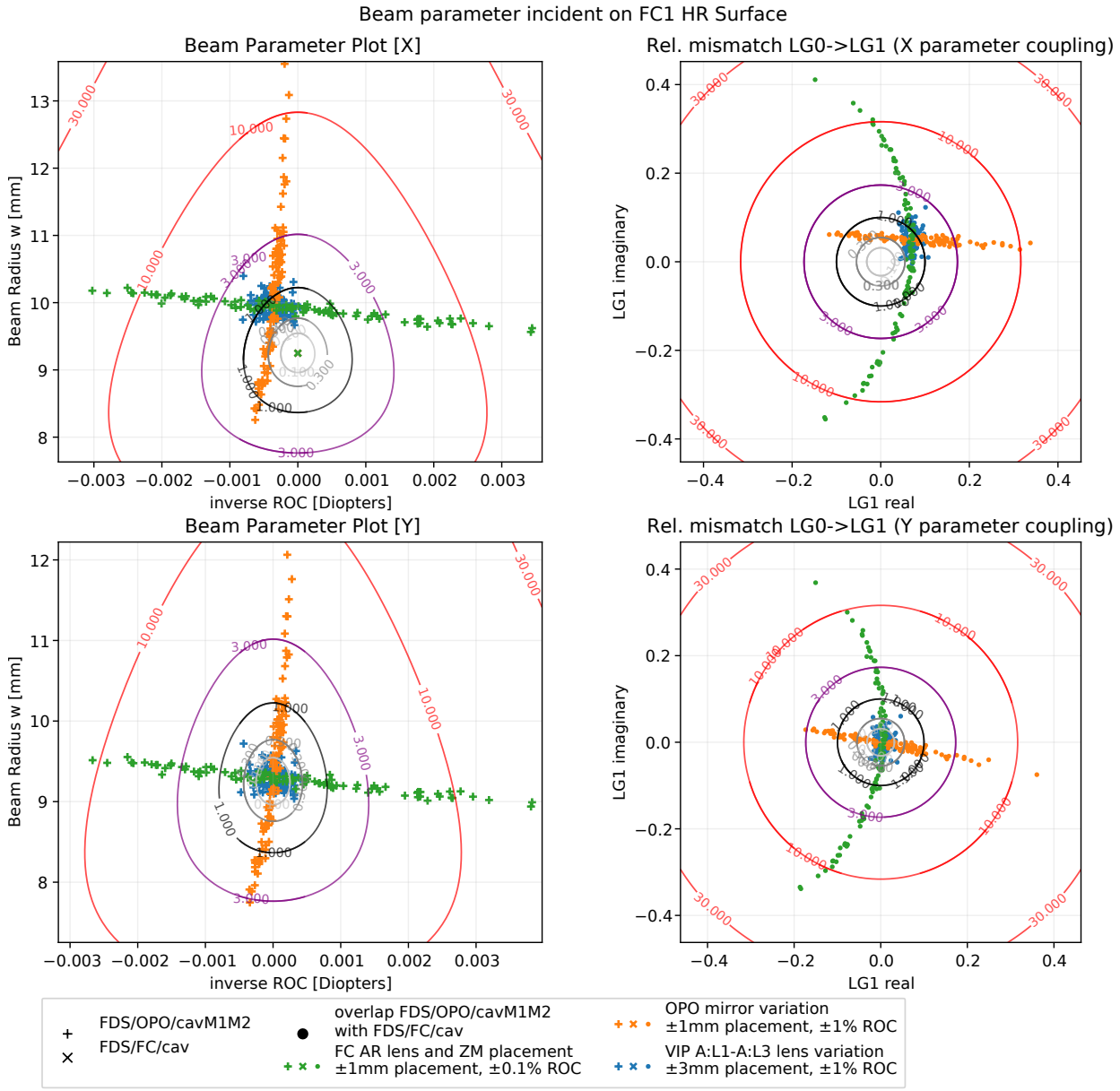

Figure 30: Monte-Carlo with variations in sets of parameters for the OPO to filter cavity telescope. This shows that the OPO to FC path (SQZFC) lenses do not contribute strongly to mismatch. The placement and as-build uncertainties in the filter cavity (green) are strong in one dimension. Surprisingly, the OPO cavity length and optics uncertainty drives very orthogonal beam parameter uncertainty.

B Views of the HAM7 Chamber

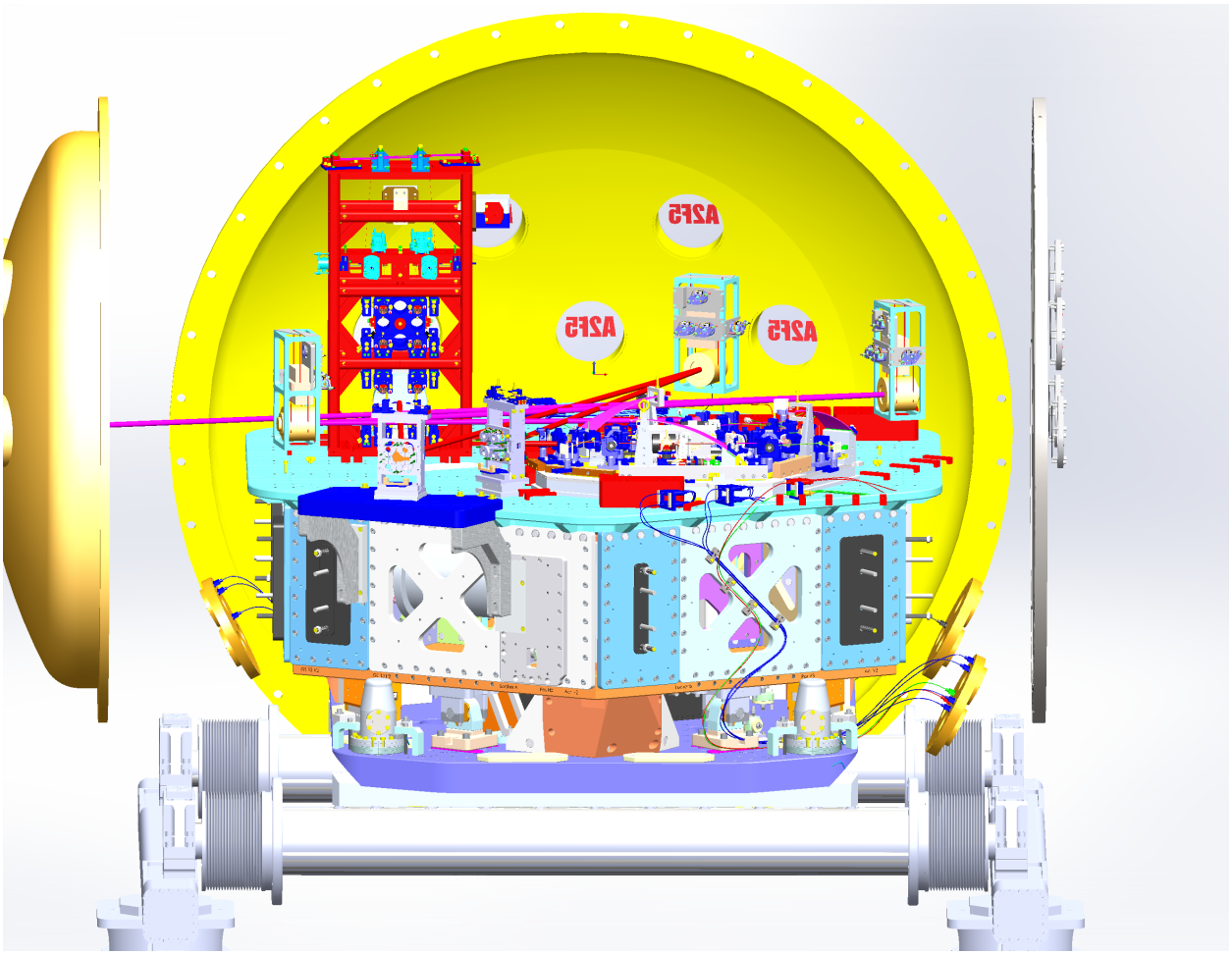

Figure 31: Views of the windows and beam clearance from ZM2 for beams routed to SQZT7

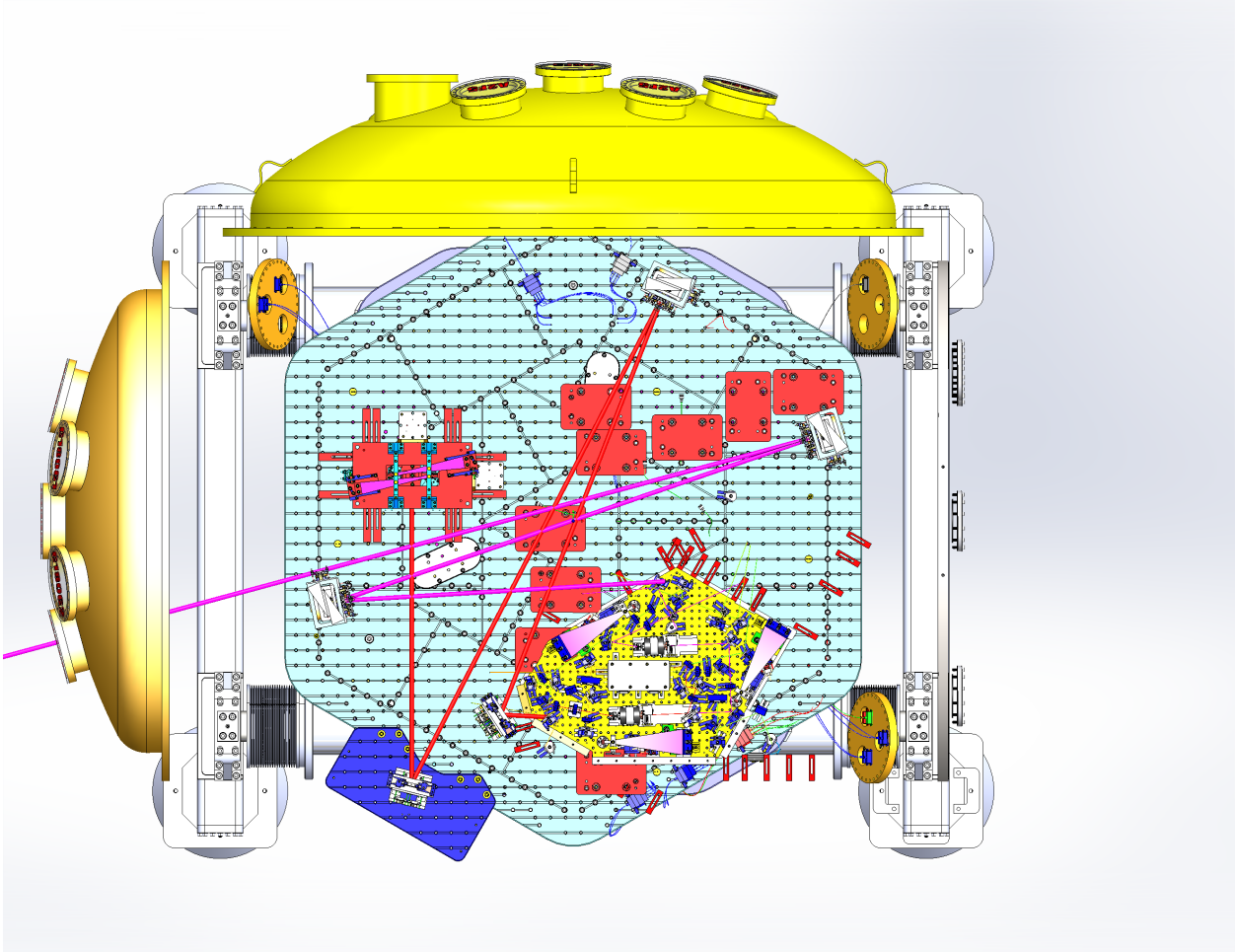

Figure 32: Overhead view to see routing around ZM2 for auxilliary beams to windows

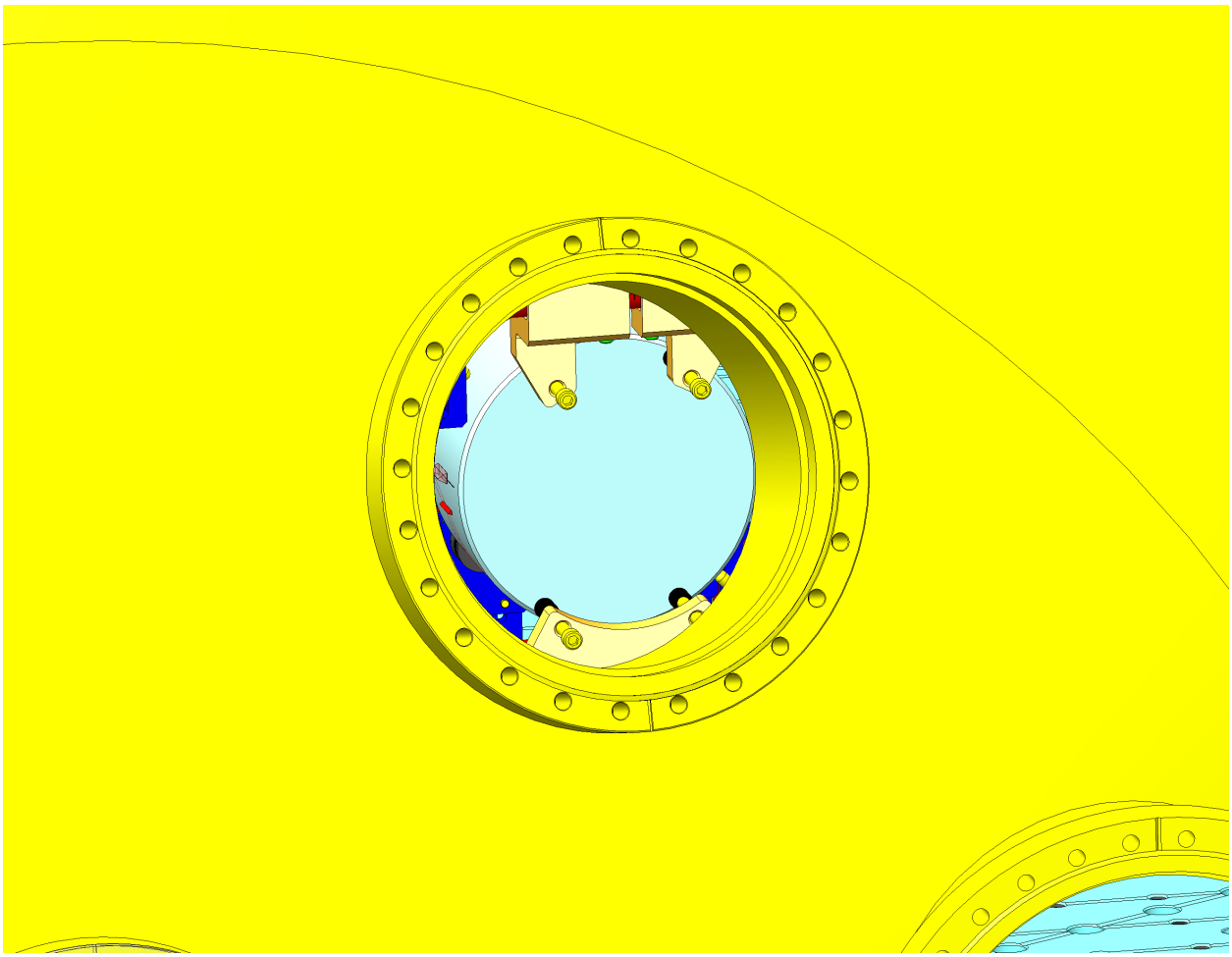

Figure 33: View of the FC1 HR surface from a camera viewport.

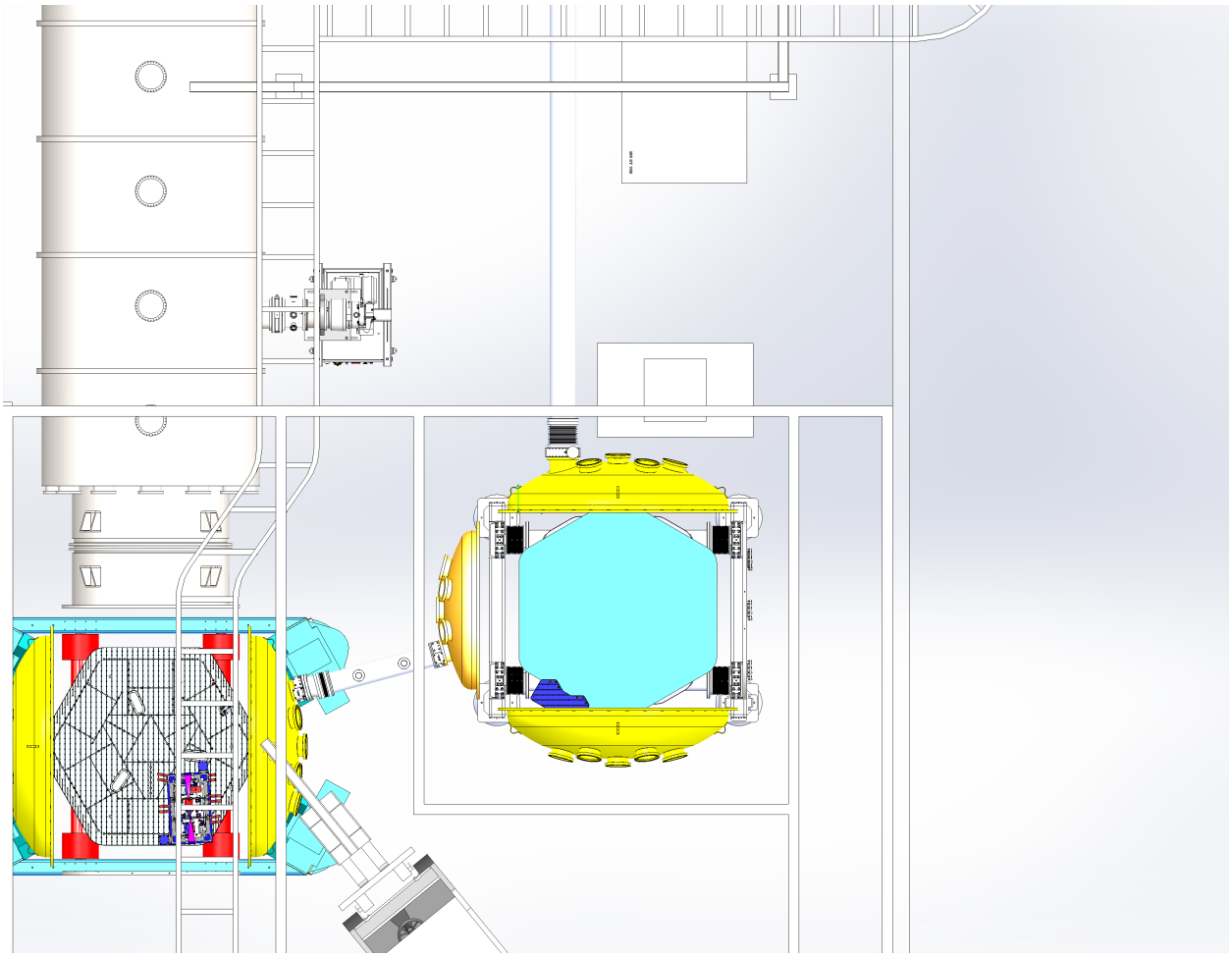

Figure 34: View of the chambers overhead to see the overall beam path and locations of optics tables.

C Current (O3) VIP Layout

Fig. 35 and Fig. 36 Show the existing layout and its implementation. The full solidworks layout is in D1500302. The solidworks model does not fully demonstrate the small scales and density of components on the implemented platform.

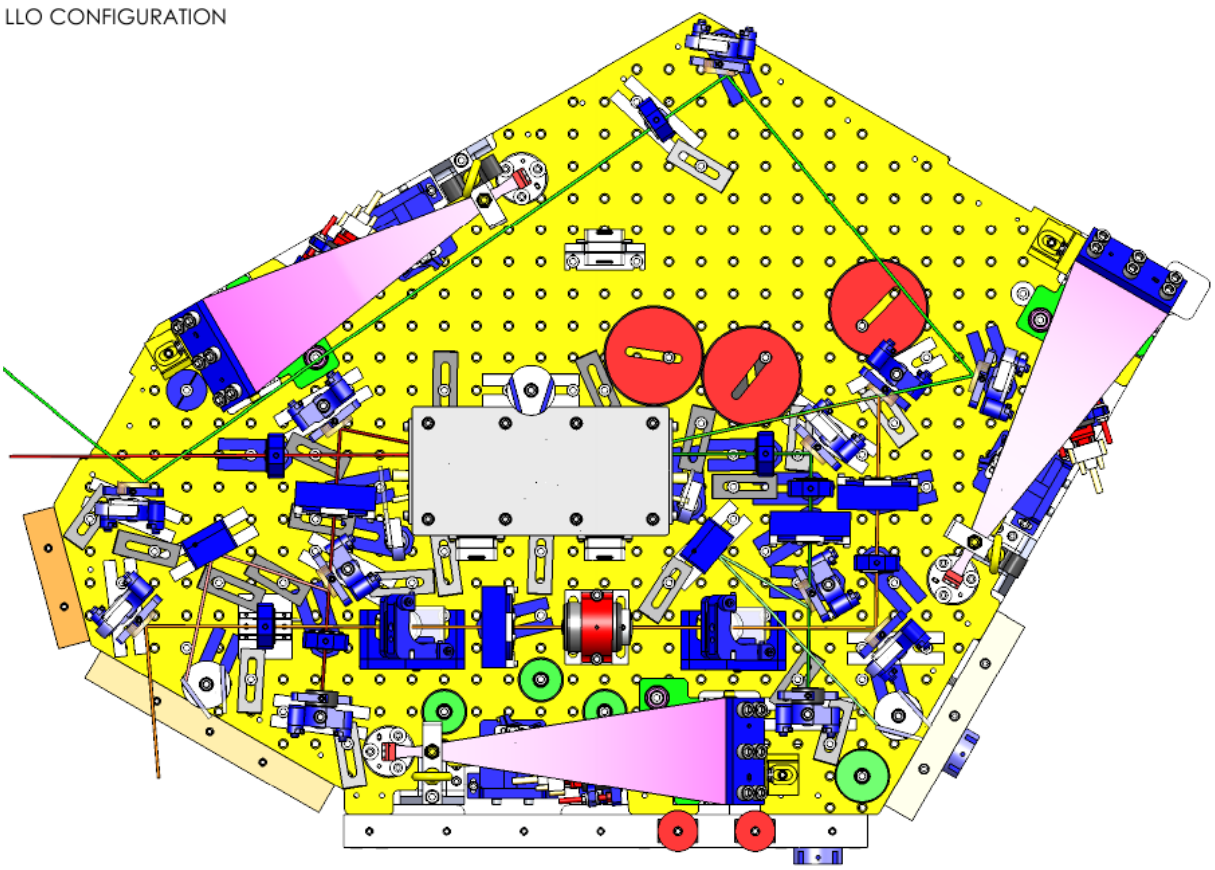

Figure 35: Solidworks rendering of the current LLO configuration of the VIP from D1500302

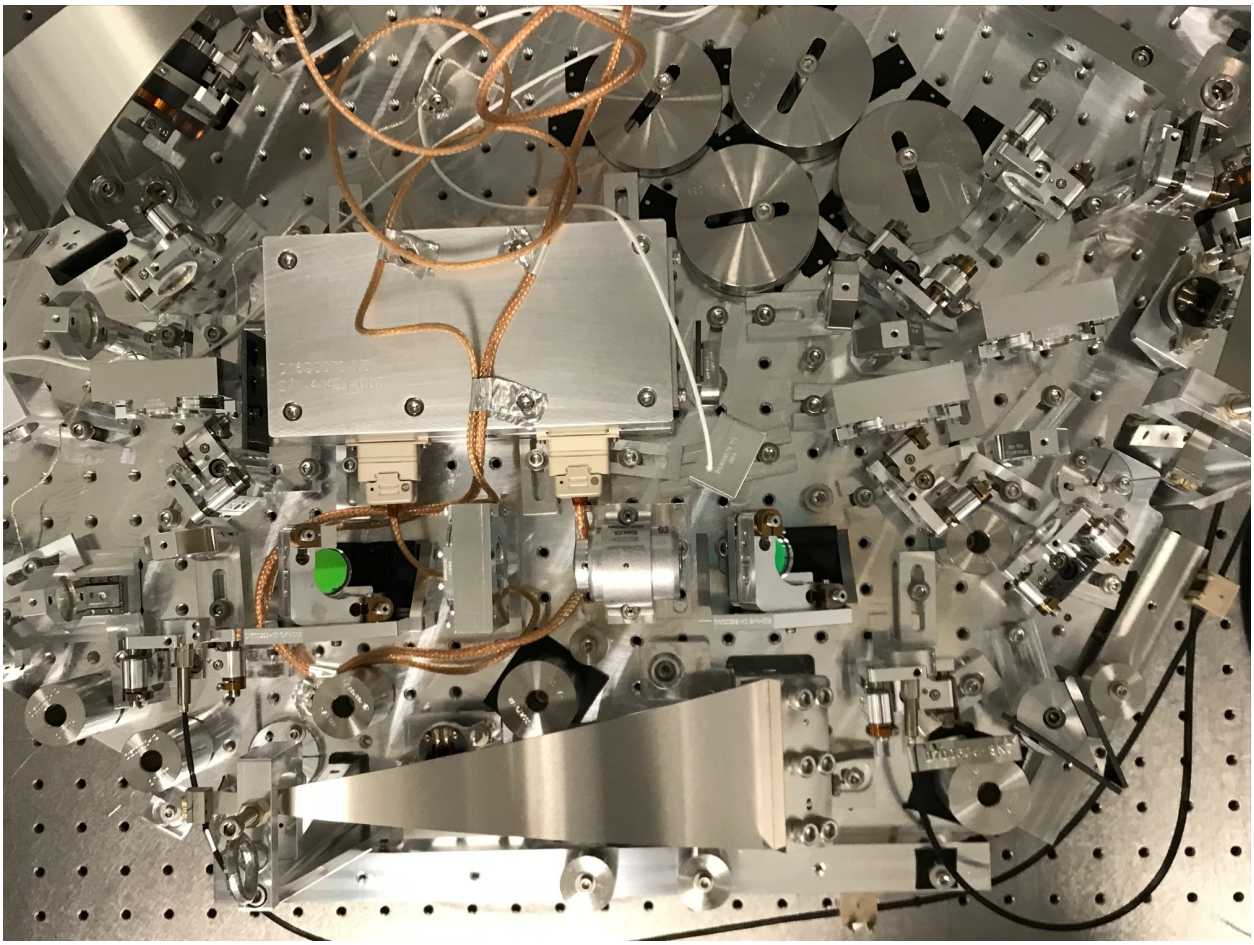

Figure 36: Top-down view of the currently implemented VIP configuration at LHO.

D IFO: ARMs to OMC

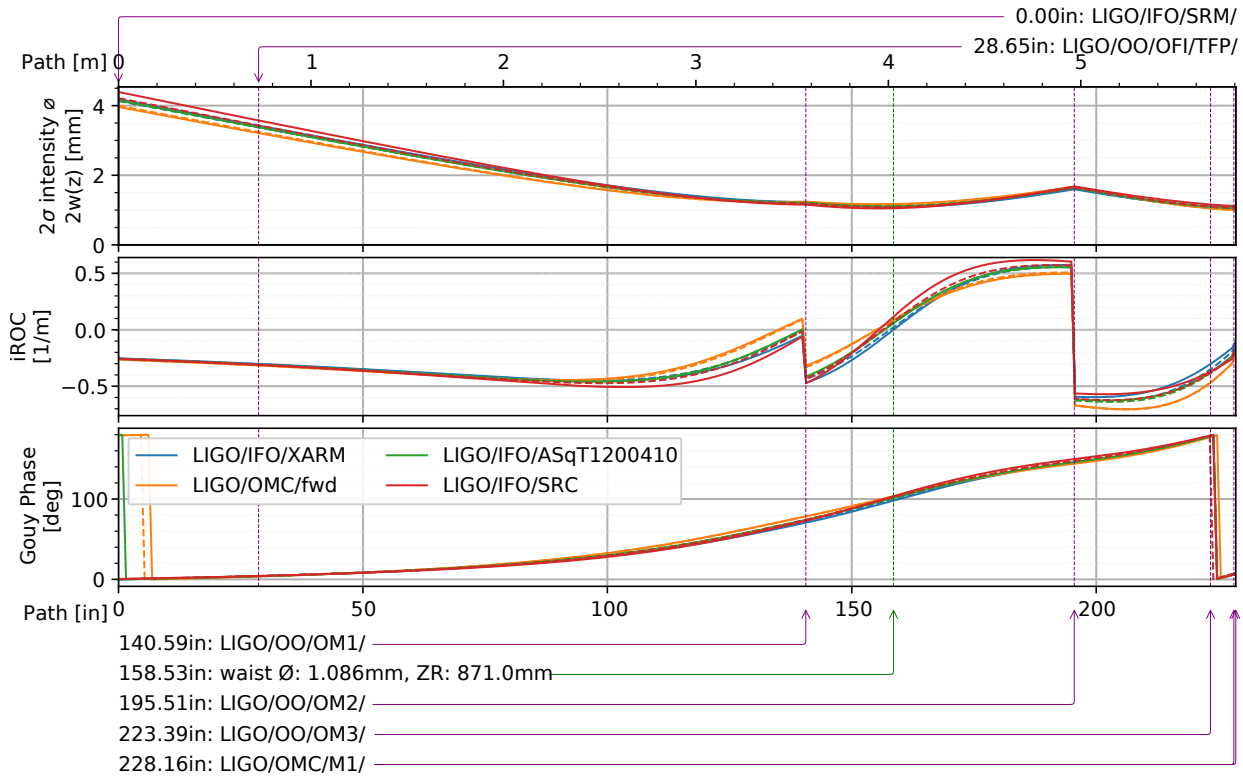

Figure 37: Beam Propagation from SRM to OMC, using the arm cavities, SRC and nominal output beam parameter from T1200410. This shows well-known implementation and modeling uncertainty in the output beam parameter.